

University of Louisville

ThinkIR: The University of Louisville's Institutional Repository

Electronic Theses and Dissertations

5-2023

Perineuronal nets are not required to close the critical period for ocular dominance plasticity.

Emily Crouse
University of Louisville

Follow this and additional works at: <https://ir.library.louisville.edu/etd>



Part of the [Molecular and Cellular Neuroscience Commons](#)

Recommended Citation

Crouse, Emily, "Perineuronal nets are not required to close the critical period for ocular dominance plasticity." (2023). *Electronic Theses and Dissertations*. Paper 4071.
<https://doi.org/10.18297/etd/4071>

This Doctoral Dissertation is brought to you for free and open access by ThinkIR: The University of Louisville's Institutional Repository. It has been accepted for inclusion in Electronic Theses and Dissertations by an authorized administrator of ThinkIR: The University of Louisville's Institutional Repository. This title appears here courtesy of the author, who has retained all other copyrights. For more information, please contact thinkir@louisville.edu.

PERINEURONAL NETS ARE NOT REQUIRED TO CLOSE THE
CRITICAL PERIOD FOR OCULAR DOMINANCE PLASTICITY

By

Emily Carol Crouse

B.A., Murray State University, 2015

M.S., University of Louisville, 2020

A Dissertation

Submitted to the Faculty of the
School of Medicine of the University of Louisville
in Partial Fulfillment of the Requirements
for the Degree of

Doctor of Philosophy
in Anatomical Sciences and Neurobiology

Department of Anatomical Sciences and Neurobiology
University of Louisville
Louisville, KY

May 2023

PERINEURONAL NETS ARE NOT REQUIRED TO CLOSE THE
CRITICAL PERIOD FOR OCULAR DOMINANCE PLASTICITY

By

Emily Carol Crouse

B.A., Murray State University, 2015

M.S., University of Louisville, 2020

A Dissertation Approved on

January 27, 2023

by the following Dissertation Committee

Aaron McGee, Ph.D.

William Guido, Ph.D.

Martha Bickford, Ph.D.

Chad Samuelson, Ph.D.

Michal Hetman, M.D., Ph.D.

ACKNOWLEDGEMENTS

I would like to start by thanking my fellow lab members for the countless ways they have given me support over the years – listening to me when I was feeling happy, sad, or angry, sharing laughter with me through the good and bad times, providing me with wisdom, strength, and courage, and finally, showing me that colleagues can become family. I would also like to thank the head of the department, Dr. Guido, for supporting me during a difficult time in my life. I will always be grateful for the amount of grace I received during that time. Lastly, I would like to thank my mentor, Aaron McGee, for teaching me everything I know and providing me with the tools for success.

ABSTRACT

PERINEURONAL NETS ARE NOT REQUIRED TO CLOSE THE CRITICAL PERIOD FOR OCULAR DOMINANCE PLASTICITY

Emily C. Crouse

January 27, 2023

In the developing visual system, a transient critical period demarcates when neural circuits are most sensitive to visual experience. In the mouse, the critical period occurs between approximately postnatal day(P) 19 to 32. Closing one eye (monocular deprivation, MD) within the critical period shifts ocular dominance (OD) to be more responsive to the open eye. Nogo-66 Receptor 1 (NGR1) limits OD plasticity to the critical period yet it remains unknown how OD plasticity propagates through primary visual cortex or by which mechanisms NGR1 utilizes to confine said plasticity. In primary studies, NGR1 was selectively deleted in different cortical layers to investigate the characteristics of OD plasticity. From these studies, we conclude that L4 regulates intracortical disinhibition to gate OD plasticity in visual cortex. First, I determined that OD plasticity advances faster in L4 than L2/3 or L5 but does not rely on a canonical cortical microcircuit for expression. Second, I examined the signaling mechanisms for NGR1. I determined that NGR1 does not operate through the TROY or LINGO coreceptors. Third, I focused on the maturation of perineuronal nets (PNNs), which contain ligands for NGR1, and for which there is substantial evidence that they are involved in the closure of the critical period. These extracellular structures are enriched in chondroitin sulfate proteoglycans (CSPGs) and predominantly ensheath inhibitory interneurons expressing parvalbumin (PV). Recent work has revealed that the gene for aggrecan (*acan*), a principal neuronal CSPG, is essential for the formation of PNNs and required to close the critical period for OD plasticity. We performed a genetic dissection of the requirement of *acan* to close this critical period by combining the conditional allele for the gene with different yet overlapping drivers for expression of Cre recombinase. Drivers that eliminated *acan* only in inhibitory neurons were not

sufficient to sustain plasticity in adulthood but deletion of *acan* in all neurons permitted OD plasticity after the closure of the critical period. Therefore, we conclude that PNNs are not required to close the critical period.

TABLE OF CONTENTS

| | |
|---|------|
| ACKNOWLEDGEMENTS..... | iii |
| ABSTRACT..... | iv |
| LIST OF FIGURES..... | viii |
| CHAPTER I..... | 1 |
| INTRODUCTION AND BACKGROUND | |
| CHAPTER II..... | 6 |
| LAYER 4 GATES PLASTICITY IN VISUAL CORTEX INDEPENDENT OF A CANONICAL MICROCIRCUIT | |
| Introduction..... | 6 |
| Methods..... | 9 |
| Results..... | 12 |
| Discussion..... | 17 |
| CHAPTER III..... | 20 |
| TROY AND LINGO ARE NOT CO-RECEPTORS THAT TRANSDUCE SIGNAL BY NGR1 TO LIMIT VISUAL PLASTICITY | |
| Introduction..... | 20 |
| Methods..... | 21 |
| Results..... | 24 |
| Discussion..... | 27 |
| CHAPTER IV..... | 28 |
| PERINEURONAL NETS ARE NOT REQUIRED TO CLOSE THE CRITICAL PERIOD FOR OD PLASTICITY | |
| Introduction..... | 28 |
| Methods..... | 29 |

| | |
|-------------------------------|----|
| Results..... | 34 |
| Discussion..... | 38 |
| CHAPTER V..... | 41 |
| SUMMARY AND FUTURE DIRECTIONS | |
| REFERENCES..... | 43 |
| CURRICULUM VITAE..... | 53 |

LIST OF FIGURES

| | |
|---|----|
| Figure 2-1. Design of the <i>ngr1</i> flx conditional allele and selective loss of <i>ngr1</i> in forebrain is sufficient to retain OD plasticity in adult mice as observed in the constitutive mutant mouse..... | 13 |
| Figure 2-2. OD plasticity is first detectable in L4 in juvenile WT and adult <i>ngr1</i> flx/flx; <i>L4-Cre</i> mice..... | 14 |
| Figure 2-3. CBI scores, OD histograms, and cumulative distributions for juvenile WT mice and adult <i>ngr1</i> flx/flx; <i>L4-Cre</i> mice after 0,2, and 4, days of MD..... | 16 |
| Figure 2-4. OD plasticity in L5 does not require OD plasticity in L2/3..... | 17 |
| Figure 3-1. A schematic of the ligands and co-receptors for NGR1..... | 25 |
| Figure 3-2. <i>Troy</i> ^{-/-} mice, <i>lingo</i> ^{-/-} mice, and <i>troy</i> ^{-/-} ; <i>lingo</i> ^{-/-} do not phenocopy the recovery of acuity observed in <i>ngr1</i> ^{-/-} mice after LTMD..... | 26 |
| Figure 3-3. Adult <i>troy</i> ^{-/-} mice and <i>troy</i> ^{-/-} ; <i>lingo</i> ^{-/-} mice do not display OD plasticity after 4 days of MD..... | 26 |
| Figure 4-1. <i>Acan</i> is required in cortical inhibitory neurons for the formation of PNNs..... | 34 |
| Figure 4-2. Deleting <i>acan</i> in cortical inhibitory neurons abolishes enrichment of aggrecan around cell soma except for a small population in layer 5..... | 35 |
| Figure 4-3. Visual acuity is normal in <i>acan</i> flx mice alone, or in combinations with Cre drivers that abolish PNNs..... | 36 |
| Figure 4-4. The critical period closes around P32..... | 37 |
| Figure 4-5. OD plasticity in critical period (CP) WT, adult WT, adult <i>acan</i> flx/flx mice alone and with different Cre drivers..... | 38 |

CHAPTER I

INTRODUCTION AND BACKGROUND

Neural plasticity both increases and decreases as a function of age. During development, immature brain circuits are dominated by excitatory inputs and do not express plasticity. As age increases, inhibitory circuits mature, and a period of high plasticity is induced termed either a critical period or a sensitive period. Plasticity then declines with age as inhibitory circuits continue to mature and brake-like factors become dominant. The neural stability that follows the 'critical' period or sensitive period consolidates functional circuitry yet also inhibits large-scale adaptations to dysfunctional inputs acquired during development or thereafter¹. Based on this information, it is imperative to understand how genes control the developmental critical or sensitive period and if it is possible to use these mechanisms to reinstate plasticity in adulthood.

A critical or sensitive period is the peak time during development in which neural circuitry is sensitive to experience². The main difference between the two types of developmental periods is that a sensitive period is a time window in which development is more easily achieved whereas a critical period has a specific time window in which certain development may occur. For example, Konrad Lorenz established the concept of a critical period through his studies of filial imprinting in graylag geese. Through his work, he demonstrated that a newly hatched gosling would imprint on him if he was the first moving object the animal encountered, but this bond only developed during a brief critical period of a few hours after hatching³. Alternatively, an example of a sensitive period is the development of binaural auditory cues in barn owls. When subjected to chronic monaural occlusion, young barn owls are able to adjust to abnormal binaural cues and learn sound localization for up to 8 weeks of age⁴. However, when barn owls above the age of 8 weeks are placed in an enriched environment, the ability to adjust to sound localization and the

ability to recover to normal cues extends into later periods of life, indicating a sensitive period rather than a critical period for auditory cues^{5,6}.

As exemplified above, different species have unique timelines for peak plasticity. Further, each sensory system, as well as different areas of the brain, within a single population have differing timelines for peak plasticity. For example in the mouse model, somatosensory and auditory cortex critical periods open and close between postnatal day (P)10 and P17 while the window for primary visual cortex opens at P19 and closes around P32^{1,7}.

Despite the differences in critical period function, timing, duration, and between species, the mouse is a premier model to study the underlying mechanisms of developmental plasticity. First, the use of genetic manipulation and tracing in the mouse has allowed identification of signaling pathways and ultimately, changes in circuitry associated with critical periods⁸. Second, the mouse visual system is easily accessible and allows for the use of measurement techniques that can't be used for other systems⁸. Last and most important, there is a general conservation of visual neural circuitry across mammals⁸.

Within the primary visual system of mammals, experience drives comparable changes to both anatomical and physiological properties, including shifts in the projections from the thalamus to the visual cortex and shifts in the response properties of cortical neurons, respectively^{9,10}. More specifically, neurons within the retina converge on the optic chiasm and then project to the dorsal lateral geniculate nucleus (dLGN) of the thalamus. In the mouse, most axons cross the optic chiasm, giving the mouse a reduced ipsilateral projection compared to predatory mammals, such as primate or cat¹¹. Within the dLGN, axons from each eye innervate eye-specific domains that are separated into layers. The primate and cat have 6 and 3 layers, respectively, while the mouse has a small ipsilateral patch surrounded by a larger contralateral domain. Axons within the dLGN then project to primary visual cortex¹¹. This conservation of circuitry between mammals has led the mouse model to become a standard system to study the underlying mechanisms of activity-dependent plasticity.

One way to study plasticity in the mouse model is to manipulate the conserved visual circuitry by inducing amblyopia. Amblyopia, or lazy eye, is a visual disorder caused by abnormal vision during a critical or sensitive period¹. The severity of amblyopia depends on the age at initiation; the disorder will be more severe if induced throughout the developmental critical period. It also depends on the type of asymmetry that occurs, such as unequal alignment, unequal refractive error, or form deprivation¹. Form deprivation, or monocular deprivation (MD), is commonly used to induce amblyopia and ultimately, to study plasticity.

MD is achieved by eyelid suture which significantly occludes the patterned visual input to one eye. Across species, MD triggers both structural and functional changes that alter the visual properties of acuity and ocular dominance (OD)¹. Visual acuity is the ability of the eye to distinguish details at a given distance. Not only does MD impair acuity, long-term MD (LTMD) can permanently alter acuity¹². Alterations in visual acuity are associated with shifts in OD, which is defined as the tendency to prefer visual input from one eye over the other. MD shifts the OD of binocular neurons away from the deprived eye and toward the open eye, resulting in a reduction of the deprived-eye acuity and an alteration of the circuitry in the visual system¹³.

In rodents, neurons in primary visual cortex exhibit a strong bias toward the contralateral eye. As stated above, primate and cat thalamus are segregated into eye specific columns, while the mouse has a small ipsilateral patch nestled inside a larger contralateral patch¹¹. The process for eye-specific columns in the dLGN is triggered by spontaneous activity from retinal waves before birth. This activity is crucial for the development of the eye-specific segregation of inputs to the dLGN, which project to primary visual cortex to form OD columns in the primate and cat¹⁴. Due to this organization, cat and primate visual cortical neurons near one another share functional selectivity. In the mouse, no such organization has been observed and neurons in primary visual cortex share little functional selectivity^{7,10}. Despite these differences in functional architecture and that eye-specific segregation occurs before birth, OD and visual acuity can be manipulated in primate, cat, and rodent with MD during postnatal development.

Visual plasticity for these properties is considered a sensitive period, as the capacity for OD plasticity exists in adulthood, but it is described within the field as a critical period and I will continue to refer to it as such moving forward. Adult plasticity is functionally different from juvenile plasticity for a number of reasons. First, the adult shift in OD is slower, smaller, and requires a longer deprivation¹⁵. Second, juvenile plasticity requires a depression of deprived eye responses for a subsequent increase in response from the nondeprived eye whereas adult plasticity may not require the initial depression of the deprived eye¹⁵. Last, adult plasticity may be restricted to supragranular and infragranular lamina in primary visual cortex¹. These differences show that plasticity in adulthood is less robust and less efficient at adapting to change than juvenile plasticity.

Overall, discordant vision during development leads to impoverished and sometimes permanently altered visual performance in adulthood. If plasticity can be reinstated in adulthood, eye dominance can be rectified and visual performance improved¹¹. Increasing evidence in the field for developmental plasticity demonstrates that removing specific molecular 'brakes' reinstates plasticity and promotes recovery from amblyopia in adulthood. This list of molecules includes nogo-66 Receptor 1 (NGR1). NGR1 comprises several leucine-rich repeats (LRRs) followed by a glycosyl-phosphatidylinositol (GPI) lipid anchor, implying the necessity of a co-receptor. NGR1 also binds to a number of ligands expressed by both neurons and oligodendrocytes¹⁶⁻¹⁸. Most importantly, NGR1 limits plasticity to the critical period for both OD and visual acuity. Stephany and colleagues demonstrated that NGR1 'knock-out' (KO) mice show a spontaneous but gradual recovery of visual acuity over 7 weeks following LTMD. MD was performed for the duration of the critical period and several weeks of normal vision following the LTMD were required to see improvement¹¹. In the same study, NGR1 KO mice retain developmental plasticity as adults. While adults require up to 8 days of MD to demonstrate OD plasticity, juveniles and NGR1 KO mice demonstrate OD plasticity after 4 days of MD¹¹.

Though it is known that NGR1 is involved in developmental plasticity, it remains unclear how OD plasticity within visual circuitry propagates through primary visual cortex or how NGR1

limits plasticity to the critical period. Here I investigate OD plasticity across different layers in primary visual cortex through selective deletion of NGR1 as well as potential co-receptors and a likely ligand through which NGR1 limits plasticity to the critical period.

CHAPTER II

LAYER 4 GATES PLASTICITY IN VISUAL CORTEX

INDEPENDENT OF A CANONICAL MICROCIRCUIT

Introduction

A critical period demarcates when cortical circuits are most sensitive to experience². In the mouse, the critical period extends from P19 – P32¹⁹. Abnormal vision during this period can permanently alter visual circuitry. Experiments performed in cat, rat, and mouse reveal that brief MD during the critical period shifts OD, or eye preference, towards the nondeprived eye^{13,19–21}. LTMD that spans the critical period results in permanent deterioration in OD¹⁰. Though synaptic and structural mechanisms have been proposed to contribute to OD plasticity, it remains unclear how visual experience alters these properties and drives enduring changes within visual circuitry^{10,22}.

While OD plasticity peaks during the postnatal critical period, it can persist into adulthood. In juvenile plasticity, the primary observation from a short-term MD is a reduction of functional strength of deprived eye responses^{19,23}. Accordingly, MD disrupts the balance of excitatory and inhibitory input to individual binocular neurons, causing suppression of parvalbumin (PV)-expressing inhibitory interneurons²⁴. This initial depression of deprived eye responses is followed by a slow, strengthening of open eye responses^{25–27}. This feature of juvenile plasticity is consistent with a role in the developmental refinement of cortical circuitry for binocular vision¹⁵.

Adulthood plasticity differs from juvenile plasticity. Whereas juvenile plasticity contributes to developmental rewiring, adult plasticity is primarily a compensatory process to maintain activity levels in adult visual cortex¹⁵. There are two key features that distinguish adult from juvenile plasticity: First, the shift in OD following MD is smaller and necessitates a longer duration of deprivation. While juveniles require 4 days of MD to produce an OD shift, adults require 7 days¹⁵.

Second, it does not require initial depression of deprived eye responses for the strengthening of nondeprived eye responses. In fact, after 7 days of MD, there is a transient and slight loss of responsiveness of the deprived eye and a delayed potentiation of responses of both eyes¹⁵.

Despite these differences, OD plasticity can be enhanced through inhibitory, environmental, and molecular mechanisms through which adult mice exhibit plasticity like that of juvenile mice. Induction of the critical period requires the maturation of specific inhibitory circuits. A precocious opening of the critical period can be induced through this mechanism by activating inhibitory γ -aminobutyric acid (GABA)_A receptors with allosteric modulators or promoting early maturation of PV-expressing inhibitory neurons^{23,28–32}. Similarly, proteins that regulate synaptic strength and/or number are saturated at excitatory synapses onto PV interneurons and impact the timing of the critical period³³. For example, mice lacking the neuronal activity-regulated pentraxin (NARP) protein fail to initiate a critical period. This failure to initiate can be rescued by enhancing the inhibitory output or excitatory drive onto PV-expressing inhibitory interneurons^{33,34}.

Similar to the requirement of inhibitory circuit maturation to open the critical period, a further increase in inhibition is required to close the critical period. Thus, the critical period can be reopened in adulthood by pharmacologically reducing inhibitory output, such as with the use of the serotonin-specific reuptake inhibitor fluoxetine, or by manipulation of circuits that regulate inhibitory interneurons^{35–38}. These disinhibitory circuits transiently suppress other inhibitory interneurons to promote plasticity in adulthood. For example, both locomotion and auditory discrimination tasks activate vasoactive intestinal peptide (VIP)-expressing interneurons, enhance activity in primary visual cortex, and promote adult plasticity by increasing inhibition onto other interneuron subtypes that target pyramidal neurons^{35–37}.

Another example of ways to alter inhibitory circuitry that reactivates critical period plasticity is through environmental enrichment or manipulation. Environmental enrichment increases histone H3 acetylation, reduces expression of PV and glutamate decarboxylase (GAD) 67 within inhibitory neurons in primary visual cortex, and weakens GABA signaling^{39–41}. Dark exposure decreases excitability of PV interneurons thus reactivating juvenile-like plasticity in adulthood. This reactivation can be reversed by increasing the strength of their excitatory inputs⁴².

Finally, there is evidence that removing molecular brakes in adulthood can promote OD plasticity. A primary model representing the physical barriers to OD plasticity are perineuronal nets (PNNs). PNNs are the latticework of the extracellular matrix, composed of chondroitin sulfate proteoglycans (CSPGs), mature as the critical period closes, and are highly enriched around PV interneurons^{43–45}. Disruption of these PNNs enables OD plasticity in adulthood. Moreover, mice lacking NGR1, a receptor for chondroitin sulfate proteoglycans, also retain OD plasticity into adulthood^{18,46,47}. Overall, disinhibitory circuits may be a primary mechanism for permitting OD plasticity in adulthood, but it remains unknown where within visual circuitry that these manipulations are operating to re-open the critical period in adulthood.

Further, it remains controversial how OD plasticity emerges and spreads through primary visual cortex. In one study performed in kittens, one day of MD shows rapid extragranular plasticity whereas the binocularity of layer 4 is maintained⁴⁸. In a separate study performed in mice, OD plasticity was shown to occur simultaneously in layers 2/3 and 4 but failed to measure OD plasticity in layer 5⁴⁹. Examining how OD plasticity is controlled across different cortical layers may provide insight into what limits cortical plasticity within visual circuitry.

In this study, the *ngr1* gene, as mentioned above, was used to explore the layer-specific mechanisms of OD plasticity. Not only is *ngr1* required to close the critical period, OD plasticity in *ngr1*-deficient adult mice (P60-P90) is indistinguishable from that of juvenile WT mice (P19-P32)⁵⁰. First, 4 days of MD yields a maximal shift in eye dominance towards the non-deprived eye for both juvenile WT mice and *ngr1*-deficient adult mice^{19,46,47}. Second, OD plasticity is resistant to benzodiazepines and barbiturates in both juvenile WT mice and *ngr1*-deficient adult mice^{23,46,50,51}. Third, MD promotes disinhibition within cortical circuitry that is mediated by a reduction of excitatory drive onto PV-interneurons in both juvenile WT mice and *ngr1*-deficient adult mice^{50,52,53}. Due to these similarities between juvenile and *ngr1*-deficient OD plasticity, *ngr1* was selectively deleted within different cortical layers to investigate the characteristics of OD plasticity.

Methods

Mice

Both the constitutive *ngr1* (-/-) and conditional *ngr1 flx/flx* mouse strains have been characterized^{54,55}. These strains had been repeatedly backcrossed onto the C57Bl6J background to at least F8. Subsequently, the *ngr1 flx/flx* line was backcrossed against C57Bl6J with either the *CamK2a-Cre* (L2-6-Cre) or *Scnn1a-Cre* (L4-Cre) which were imported from Jackson Labs (strain numbers 005359 and 009613, respectively). Wild-type mice are C57Bl6J (The Jackson Laboratory, strain 00664). The specificity for each Cre driver line was validated by crossing each line to the Cre reported line *Ai14* (tdTomato) (The Jackson Laboratory, strain 007914). Experiments and procedures were performed on both adult male and female mice blind to genotype and/or treatment condition. Mice were group housed and maintained on a 12-hr light/dark cycle under standard housing conditions. For experimental and control groups including the *ngr1 flx/flx* line, experiments were performed on littermates. Genotyping was performed using custom primer sets for polymerase chain reaction (PCR) amplification with REDExtract-N-Amp PCR kit (XNAT, Sigma). All mice were genotyped for germline recombination of the *ngr1 flx* allele with custom primer sets. Mice with germline recombination were ejected from the study.

Monocular Deprivation (MD)

One eye was closed on P25-27, or P60-90 using a single mattress suture tied with 6-0 polypropylene monofilament (Prolene 8709H; Ethicon) under brief isoflurane anesthesia (2%) for durations described. The knot was sealed with cyanoacrylate glue. Upon removing the suture, the eye was examined under a stereomicroscope and animals with scarring of the cornea were eliminated from the study.

Electrophysiological Recordings in Visual Cortex

Recordings and analysis were performed blind to genotype or drug treatment. Methods were adapted from previously published methods⁵⁶. In brief, mice were anesthetized with isoflurane (4% induction, 1-2% maintenance in O₂ during surgery). The mouse was placed in a stereotaxic

frame and body temperature was maintained at 37°C by a homeostatically-regulated heat pad (TCAT-2LV, Physitemp). Dexamethasone (4 mg/kg s.c.; American Reagent) was administered to reduce cerebral edema. The eyes were flushed with saline, and the corneas were protected thereafter by covering the eyes throughout the surgical procedure with ophthalmic ointment (Puralube, Dechra Pharmaceuticals), and with frequent application of saline. A craniotomy was made over visual cortex in the left hemisphere and a custom-designed aluminum head bar was attached with cyanoacrylate glue or Metabond over the right hemisphere to immobilize the animal during recording. Prior to transfer to the recording setup, a dose of chlorprothixene (0.5 mg/kg i.p.; C1761, Sigma) was administered to decrease the level of isoflurane required to maintain anesthesia to 0.6%.

Recordings were made with Epoxylite-coated tungsten microelectrodes with tip resistances of 10-15 M Ω (FHC). The signal was amplified (model 3600; A-M Systems), low-pass filtered at 3000Hz, high-pass filtered at 300Hz, and digitized (micro1401; Cambridge Electronic Design). Multi-unit activity was recorded from four to six locations separated by >90 μ m in depth for each electrode penetration. In each mouse, there were four to six penetrations separated by at least 200 μ m across the binocular region of primary visual cortex, defined by a receptive field azimuth < 25°. Responses were driven by drifting sinusoidal gratings (0.1cpd, 95% contrast), presented in six orientations separated by 30° (custom software, MATLAB). The gratings were presented for 1s of each 3s trial. The grating was presented in each orientation in a pseudorandom order at least four times, interleaved randomly by a blank, which preceded each orientation once. Action potentials (APs) were identified in recorded traces with Spike2 (Cambridge Electronic Design). Only waveforms extending beyond 4 standard deviations above the average noise were included in subsequent analysis. For each unit, the number of APs in response to the grating stimuli was summed and averaged over the number of presentations. If the average number of APs for the grating stimuli was not greater than 50% above the blank, the unit was discarded. Units were classified as L2/3, L4, or L5 according to recording depth of the electrode measured from the pial surface. Units recorded between 150-300 microns were classified as L2/3, between 350-450 microns as L4, and between 500-700 microns as L5⁵⁷.

The ocular dominance index (ODI) was calculated for each unit by comparing the number of APs elicited in a given unit when showing the same visual stimulus to each eye independently. Units were assigned to one of seven OD categories (1-7) where units assigned to category 1 are largely dominated by input from the contralateral eye, and units assigned to category 7 are largely dominated by input from the ipsilateral eye¹³. To categorize each unit, the average number of APs elicited by the blank was subtracted from the average number of APs elicited by the gratings for the contralateral eye (CE) and the ipsilateral eye (IE). Next, the ODI, given by $ODI = (IE - CE)/(IE + CE)$ was calculated for each unit and assigned to OD categories 1-7 as follows: -1 to -0.6 = 1, -0.6 to -0.4 = 2, -0.4 to -0.1 = 3, -0.1 to 0.1 = 4, 0.1 to 0.4 = 5, 0.4 to 0.6 = 6, 0.6 to 1 = 7. Finally, the sum of the number of cells in each category was used to calculate the CBI for each animal with the formula: $CBI = [(n1 - n7) + (2/3)(n2 - n6) + (1/3)(n3 - n5) + N]/2N$ where N is the total number of units and n_x is the number of units with OD scores equal to x ¹⁹.

AM-251 Treatment

AM-251 was administered as previously described⁴⁹. In brief, AM-251 (Tocris, 1117) was solubilized in a vehicle solution containing 10% Tween-80 (Sigma, P1754) and 20% dimethyl sulfoxide (Sigma, 41640) at 2 mg/ml. The drug solution was formulated each day. Groups of juvenile WT mice were treated twice daily by intraperitoneal injection at 5 mg/kg for 4 consecutive days starting at P26 with either drug or a corresponding volume of vehicle solution. The first injection was concomitant with MD.

Quantification and Statistical Analysis

All statistical analyses were performed using Prism software (version 8.0, GraphPad). Group numbers are stated in the Results and Figure Legends. *N* represents the number of mice for group comparisons and units for cumulative distributions, except for Figures 4 and 5 where *n* corresponds to the number of cells. Unless otherwise stated, group comparisons were made using the Kruskal-Wallis test with Dunn's correction. The specific pairwise tests are described in the Results section. Values presented are the mean plus/minus the standard deviation.

Results

We dissected the expression requirement for *ngr1* to close the critical period by deleting the gene within different populations of excitatory neurons through a conditional allele (*ngr1 flx*). In this allele, *loxP* sites flank the second exon that contains the entire protein coding sequence of the mature receptor. Cre recombinase deletes this region to abolish the expression of NGR1 protein and to initiate the expression of enhanced green fluorescent protein (GFP) from a reporter cassette containing the splice acceptor sequence of *ngr1* exon 2 (Figure 2-1)⁵⁵. In the absence of Cre recombinase, GFP expression is not detectable by immunofluorescence staining of coronal brain sections or by immunoblot⁵⁶.

OD plasticity is expressed in V1 where inputs from monocular neurons residing in different laminae of the dLGN of the thalamus are combined. In the mouse, the separation of thalamic inputs is less distinct than in cats or primates, but relay neurons in LGN conveying information from each eye similarly converge in the binocular zone of V1. A characteristic of mice is overall greater responses to visual input from the contralateral eye^{19,58}. WT mice possess contralateral bias index (CBI) values that typically range from 0.65 to 0.75 as calculated from multi-unit electrophysiologic recordings with high impedance electrodes (10 mega-ohm or greater) across the depth of V1 (CBI = $0.68 \pm .05$, $n = 5$) (Figure 2-1)⁴⁷. Following 4-5 days of MD during the critical period (P27-32), WT mice display OD plasticity that shifts eye dominance towards the non-deprived eye (4-day MD juvenile WT, CBI = $0.52 \pm .05$, $n = 8$) ($P = .034$, Kruskal-Wallis test with Dunn's correction (KW test) for each of 3 genotypes comparing non-deprived vs. 4-day MD (Figure 2-1).

We deleted *ngr1* throughout neocortex with *CamK2a-Cre* (*L2-6-Cre*) to determine if restricting the deletion of *ngr1* to excitatory cortical neurons would permit OD plasticity in adult mice after the close of the critical period. This transgene expresses Cre recombinase in excitatory neurons in layers (L) L2 through L6 of cerebral cortex but not in thalamic nuclei⁵⁹. Adult *ngr1 flx/flx*; *L2-6-Cre* mice exhibited OD plasticity with MD (CBI = $0.41 \pm .05$; $n = 5$), and their CBI values were significantly lower than those of non-deprived *ngr1 flx/flx*; *L2-6-Cre* control mice (CBI = $.73 \pm .04$; $n = 4$, $P = .004$, KW test) (Figure 2-1). This OD plasticity is comparable to that observed in both juvenile

WT mice and adult *ngr1*^{-/-} mice (non-deprived KO CBI = .65 ± .04 vs. 4-day MD KO CBI = .42 ± .11, *P* = .024, KW test) (Figure 2-1)^{19,46}.

Juvenile WT mice display OD plasticity in every cortical layer¹⁹. To measure OD plasticity in different cortical layers, we examined ODI scores at recording depths from the pial surface corresponding to L2/3 (150-300 microns), L4 (350-450 microns), and L5 (550-750 microns) (Figure 2-1)⁵⁷. Comparing the cumulative distributions of ODI scores for non-deprived *ngr1* *flx/flx*; *L2-6 Cre* mice and *ngr1* *flx/flx*; *L2-6 Cre* mice receiving 4 days of MD revealed significant OD plasticity in each cortical layer (*P* < .0001, KW test for each layer between non-deprived and 4-day MD groups) (Figure 2-1). Thus, selective deletion of *ngr1* in excitatory cortical neurons is sufficient to permit OD plasticity throughout V1 that is otherwise confined to a developmental critical period.

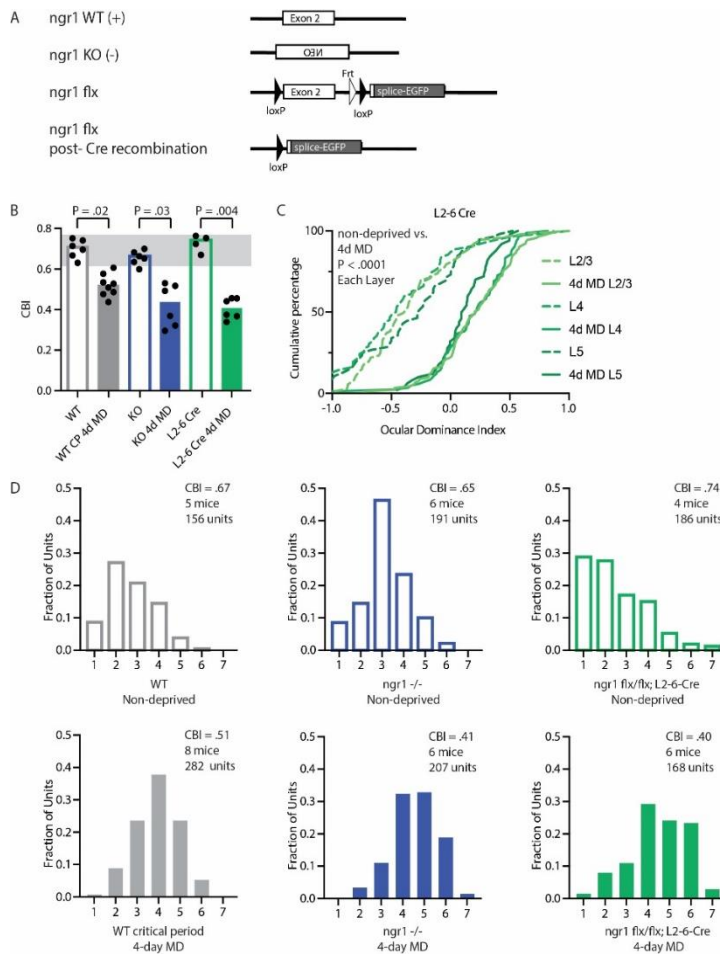


Figure 2-1. Design of the *ngr1* *flx* conditional allele and selective loss of *ngr1* in forebrain is sufficient to retain OD plasticity in adult mice as observed in the constitutive mutant mouse. Schematic of the *ngr1* WT, KO, and *flx* allele before and after Cre-mediated recombination. In the *flx* allele, exon 2 is flanked by loxP sites and an expression cassette for GFP is positioned after the 3' untranslated region (UTR). Cre recombinase activity excises this essential exon and promotes expression of GFP under control of the *ngr1* promoter. **(B)** Contralateral Bias Index (CBI) scores for non-deprived adult WT mice (WT, n=6), juvenile WT mice following 4 days of monocular deprivation (4d MD) (WT CP 4d MD, n=8), adult non-deprived *ngr1*^{-/-} mice (KO, n=6), adult non-deprived *ngr1* *flx/flx*; *L2-6-Cre* mice (L2-6 Cre, n=4), and adult *ngr1* *flx/flx*; *L2-6-Cre* mice following 4d MD (L2-6 Cre 4d MD, n=6). Individual mice are represented as circles. The bar represents the mean of each group. The range of typical CBI values for non-deprived adult WT mice are demarcated by the grey rectangle. KW test comparing non-deprived and 4d MD for each genotype. **(C)** Cumulative distributions of units for non-deprived adult WT mice (WT, n=6), juvenile WT mice following 4 days of monocular deprivation (WT CP 4d MD, n=8), adult non-deprived *ngr1*^{-/-} mice (KO, n=6), adult non-deprived *ngr1* *flx/flx*; *L2-6-Cre* mice (L2-6 Cre, n=4), and adult *ngr1* *flx/flx*; *L2-6-Cre* mice following 4d MD (L2-6 Cre 4d MD, n=6). MD yields a significant shift in the distribution of recorded units for each layer (*P* < .0001, KW test comparing non-deprived and 4d MD for each layer). **(D)** 7-point scale OD histograms for non-deprived WT, WT critical period 4-day MD, non-deprived KO, KO 4-day MD, non-deprived L2-6 Cre, and L2-6 Cre 4-day MD.

OD plasticity advances faster in L4 than L2/3 or L5 in mice

Electrophysiologic recordings in kittens has revealed that L2/3 and L5 display more rapid OD plasticity than L4 following brief MD⁴⁸. The progression of OD plasticity by layer in mouse is less clear, although juvenile WT mice display OD plasticity in every cortical layer¹⁹. Multi-unit electrophysiologic recordings to measure OD plasticity in mice indicate that 4 or more days are required to yield the maximal shift in eye dominance¹⁹. In contrast, a more recent study has reported that L2/3 and L4 display near complete OD plasticity simultaneously with 1 day of MD⁴⁹.

To discriminate between these disparate outcomes, we examined the effects of 2 days of MD in both juvenile WT mice (P26/27 at MD) and adult *ngr1 flx/flx*; *L4-cre* mice (P60-90 at MD) that lack *ngr1* expression in L4 and sustain OD plasticity as adults similar to adult *ngr1 flx/flx*; *L2-6-cre*^{60–62} (Figures 2-2 and 2-3). We identified a partial but significant reduction in CBI values for both groups following only 2d of MD (WT, non-deprived CBI = $0.76 \pm .06$, $n = 6$; 2d MD CBI = $0.61 \pm .10$, $n = 7$, $P = .035$; MW test; *ngr1 flx/flx*, *L4-Cre* non-deprived CBI = $0.71 \pm .07$, $n = 6$; 2d MD CBI = $0.57 \pm .11$, $n = 6$, $P = .041$; MW test) (Figure 2-2).

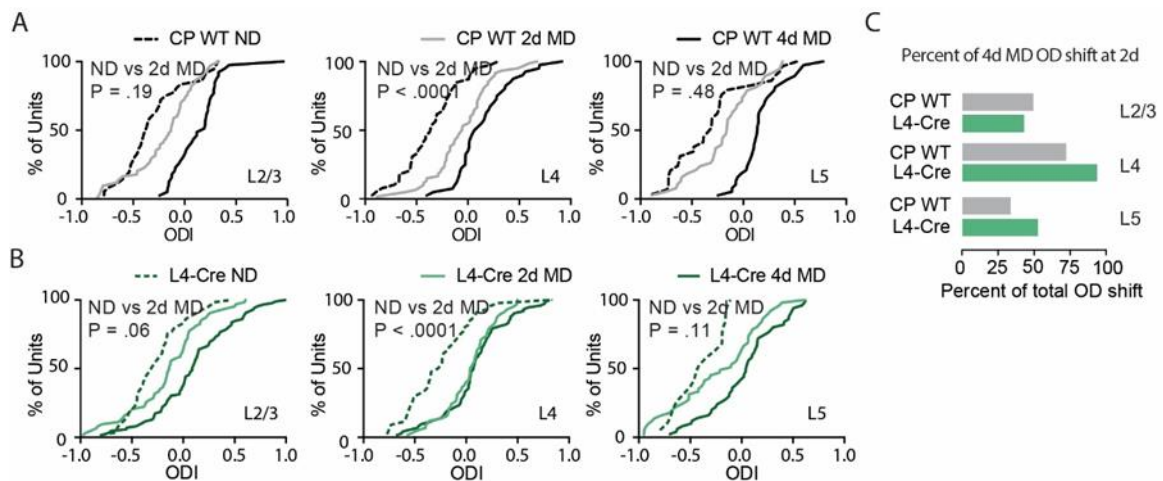


Figure 2-2. OD plasticity is first detectable in L4 in juvenile WT and adult *ngr1 flx/flx*; *L4-Cre* mice. (A) Cumulative distributions of ODI values for units in L2/3 (left), L4 (middle), and L5 (right), for non-deprived critical period (CP) WT mice (ND, dashed line) and following 2 days of MD (2d MD, light grey line) and 4 days of MD (4d MD, dark grey). Units per layer in parentheses, L2/3: ND (36), 2d (73), 4d (39); L4: ND (39), 2d (60), 4d (40); L5: ND (29), 2d (38), 4d (38). Statistical comparison is a KW test comparing all combinations of ND, 2d MD, and 4d MD for each layer. (B) Cumulative distributions of ODI values for units in L2/3 (left), L4 (middle), and L5 (right), for non-deprived adult *ngr1 flx/flx*; *L4-Cre* mice (ND, dashed line) and following 2d MD (2d MD, light green) and 4d MD (4d MD, dark green). Units per layer in parentheses, L2/3: ND (57), 2d (63), 4d (86); L4: ND (44), 2d (58), 4d (73); L5: ND (19), 2d (51), 4d (50). Statistical comparison is a KW test comparing all combinations of ND, 2d MD, and 4d MD for each layer. (C) The percentage of the total OD shift per layer between non-deprived mice and after 4d of MD achieved by 2d of MD for both CP WT mice and adult *ngr1 flx/flx*; *L4-Cre* mice.

We evaluated cumulative distributions of the ODI scores for each cortical layer from these recordings. OD plasticity was more advanced after 2 days of MD in L4 than L2/3 or L5. The ODI scores from juvenile WT mice after 2 days of MD were significantly different from non-deprived mice in L4 but not in L2/3 or L5 ($P < .0001$, $P = .19$, and $P = .48$, respectively, KW test comparing all combinations of non-deprived, 2-day MD, and 4-day MD for each layer) (Figure 2-2). Similarly, the ODI scores from adult *ngr1 flx/flx; L4-cre* mice after 2 days of MD were significantly different from the ODI scores from non-deprived mice in L4 but not in L2/3 or L5 ($P < .0001$, $P = .06$, and $P = .11$, respectively, KW test comparing all combinations of non-deprived, 2-day MD, and 4-day MD for each layer) (Figure 2-2).

To determine the fraction of the overall OD shift following 4 days of MD that was present at 2 days of MD, we compared the medians of these cumulative distributions at 0, 2, and 4 days of MD for each layer and calculated the percentage of the overall change in ODI following 4 days MD present at 2 days of MD (Figure 2-2). In juvenile WT mice, 2 days of MD attained nearly three-quarters of the overall OD shift measured following 4 days of MD in L4, but approximately half of the overall OD shift for L2/3 and L5. In adult *ngr1 flx/flx; L4-Cre* mice, 2 days of MD attained more than three-quarters of the overall OD shift measured following 4 days of MD in L4, but again approximately half of the overall OD shift for L2/3 and L5 (Figure 2-2 and 2-3). We conclude from these experiments that OD plasticity advances faster in L4 than L2/3 or L5 in mice.

OD plasticity does not rely on a canonical cortical microcircuit

This finding that OD plasticity advances faster in L4 than L2/3 or L5 is consistent with a canonical circuit model for OD plasticity in which changes in eye dominance propagate from L4 to L2/3 to L5⁶³. A prediction of this model is that OD plasticity in L2/3 is required for OD plasticity in L5. To test this prediction, we employed pharmacology to attenuate OD plasticity in L2/3 during 4 days of MD and examined OD plasticity in L4 and L5 (Figure 2-4). AM-251 is a CB1 receptor antagonist that blocks OD plasticity in L2/3 during 1 day of MD⁴⁹. We treated juvenile WT mice with AM-251 (5mg/kg) or vehicle (10% Tween 80, 20% dimethyl sulfoxide in water) as previously reported⁴⁹, but we repeated the dosing every 12 hours for 4 days in conjunction with MD.

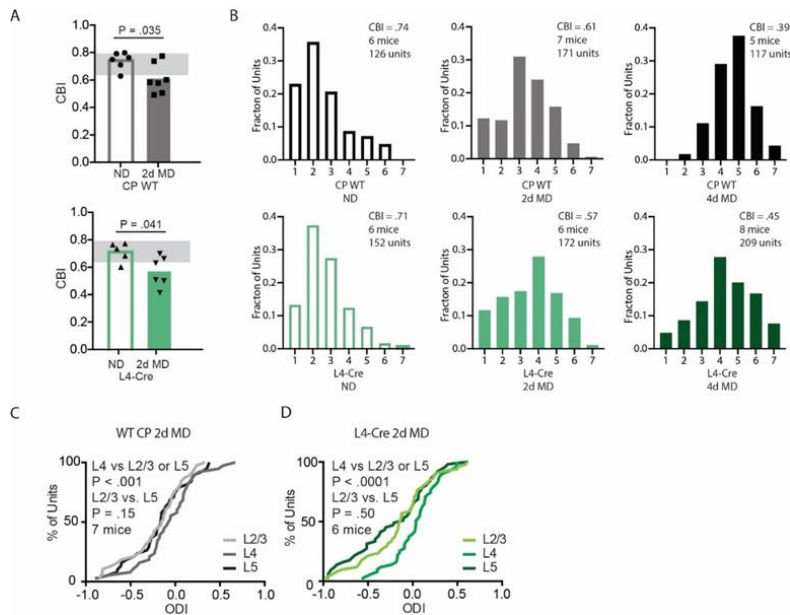


Figure 2-3. CBI scores, OD histograms, and cumulative distributions for juvenile WT mice and adult *ngr1 flx/flx*; L4-Cre mice after 0, 2, and 4, days of MD. (A) CBI scores for critical-period wild-type (CP WT) and adult *ngr1 flx/flx*; L4-Cre (L4-Cre) mice that are either non-deprived (ND) (CP WT 6 mice, L4-Cre 6 mice) or after 2 days of MD (2d MD) (CP WT 7 mice, L4-Cre 6 mice). CBI scores are significantly lower for both CP WT mice ($P=.035$) and L4-Cre mice ($P=.041$) after 2d MD relative to ND. The range of typical CBI values for non-deprived adult WT mice from Figure 2-1 are demarcated by the grey rectangle. **(B)** 7-point scale OD histograms for CP WT and L4-Cre mice at 0, 2, and 4 days of

MD. **(C)** Normalized distributions of units in L2/3, L4, and L5, from WT mice during the critical period following 2 days of MD (7 mice, at least 38 units per layer). Units from L4 are significantly different from units in L2/3 and L5 ($P < .001$) whereas units from L2/3 and L5 are not ($P=.15$, Friedman test) **(D)** Normalized distributions of units in L2/3, L4, and L5, from adult *ngr1 flx/flx*; L4-Cre mice following 2 days of MD (6 mice, at least 51 units per layer, see Figure 2-2). Units from L4 are significantly shifted from units in L2/3 and L5 ($P < .0001$) whereas units from L2/3 and L5 are similar ($P=.50$, Friedman test).

CBI values from units recorded from L2/3 were significantly different between non-deprived mice and mice receiving 4 days of MD together with injection of vehicle solution (L2/3 non-deprived vs. L2/3 4D vehicle, $P = .008$; KW test comparing non-deprived vs. 4-day MD with and without drug) (Figure 2-4). However, treatment with AM-251 during MD abolished OD plasticity in L2/3 (L2/3 non-deprived vs. L2/3 4D AM-251, $P = .99$, KW test). In contrast, OD plasticity in both L4 and L5 were unaffected. In L4, the shift in OD following 4 days of MD was similar for mice treated with either drug or vehicle relative to non-deprived controls (L4 non-deprived vs. L4 4D vehicle, $P = .004$; L4 non-deprived vs. L4 4D AM-251 treated, $P=.004$; KW test comparing non-deprived vs. 4-day MD with and without drug) (Figure 2-4). In L5, OD plasticity was similarly unaltered by drug treatment (L5 non-deprived vs. L5 4D vehicle, $P < .0001$; L4 non-deprived vs. L4 4D AM-251 treated, $P < .0001$; KW test comparing non-deprived vs. 4-day MD with and without drug) (Figure 2-4). Thus, L5 does not inherit eye dominance from L2/3 nor require OD plasticity in L2/3.

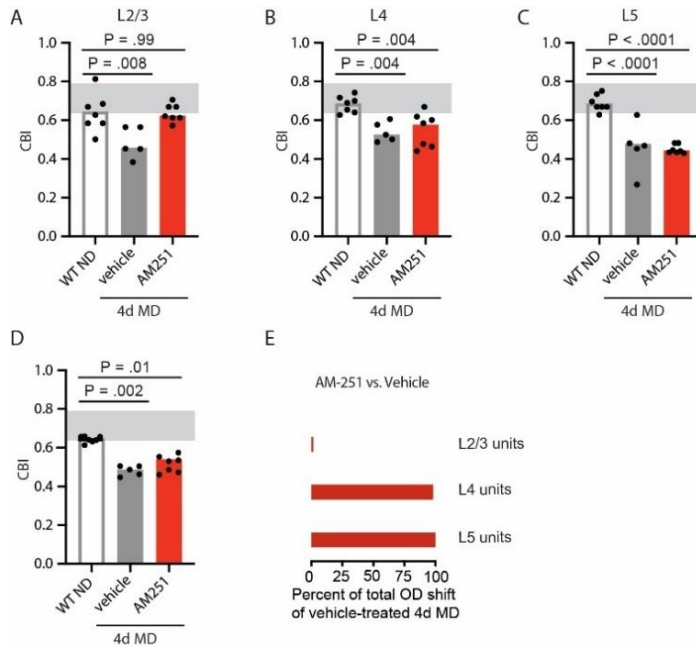


Figure 2-4. OD plasticity in L5 does not require OD plasticity in L2/3. Contralateral Bias Index (CBI) scores for critical-period wild-type (WT) mice either non-deprived (ND) (7 mice) or after 4 days (4d) of MD during treatment with AM-251 (7 mice) or vehicle (5 mice) segregated by layer. **(A)** AM-251 blocks OD plasticity in L2/3 as AM-251 treated is not significantly different from ND while vehicle treated is significantly lower ($P=.99$ and $P=.008$, respectively, KW test). **(B)** AM-251 does not affect OD plasticity in L4 as both AM-251 treated and vehicle treated are significantly different than ND ($P=.004$ for each, KW test). and **(C)** AM-251 does not affect OD plasticity in L5 as both AM-251 treated and vehicle treated are significantly different than ND ($P<.0001$ for each, KW test). **(D)** Contralateral Bias Index (CBI) scores for each mouse across all recording depths (L2/3, L4, and L5) Both AM-251 treated mice ($P=.01$) and vehicle treated mice ($P=.002$) are significantly lower than ND (K-W test). **(E)** The percentage of the total OD shift per layer between non-deprived mice and after 4 days of MD during vehicle treatment achieved by 4d MD during AM-251 treatment.

Discussion

OD plasticity by adult *ngr1* mutant mice displays several hallmarks of OD plasticity otherwise confined to a developmental critical period¹¹. Comparing the effects of MD on *ngr1* mutant mice relative to adult WT mice provides an opportunity to identify cortical circuit and signaling changes associated with OD plasticity outside the context of development when MD may have a number of effects on neural circuits, only some of which contribute to OD plasticity. For example, MD during the critical period not only alters eye dominance but also prevents the maturation of acuity by the deprived eye¹². Previously we demonstrated that recovery of eye dominance and acuity following prolonged MD are independent in the mouse, and can be rescued separately by deleting *ngr1* either in cerebral cortex and thalamus, respectively⁵⁶.

How OD plasticity emerges and propagates through cortical circuitry has proven difficult to resolve. Some of the earliest work testing the effects of very brief durations of MD (4-8 hours) on binocularity in kitten visual cortex concluded that OD plasticity occurs first in L4 and L5⁶⁴. In contrast, a subsequent study examining the effects of 1 day of MD in kittens proposed that OD plasticity advances faster in L2/3, L5, and L6, than L4⁴⁸. However, these experiments were not

identical in design. The latter study targeted recordings to the junction of eye dominance domains rather than probing uniformly across V1.

In the mouse, OD plasticity has been reported to be simultaneous but independent in L2/3 and L4⁴⁹. However, the OD plasticity in this study was unusually fast, resulting in near complete shifts in eye dominance following a single day of MD for both L2/3 and L4. In addition, these experiments employed custom-designed electrodes and an unconventional analysis method. Such rapid shifts in OD are not evident in numerous other studies^{15,19,26}, nor in our recordings where we observe that OD plasticity advanced more rapidly in L4 than L2/3 or L5 (Figure 2-2). This difference seems unlikely to be a consequence of sampling bias in our experiments because we examined a similar number of mice (7 vs. 9) and more units (133 vs. 50)⁴⁹.

OD plasticity advancing more rapidly in L4 than other layers is consistent with it propagating through a canonical cortical microcircuit. To evaluate whether OD plasticity follows this classic circuit, we employed pharmacology to prevent OD plasticity in L2/3 and examined the consequences on L5. AM-251 is a potent antagonist for the cannabinoid receptor CB1 with a K_i near 8 nanomolar⁶⁵. A single injection is sufficient to block OD plasticity in L2/3 during one day of MD⁴⁹. In acute slices, bath application of AM-251 also impairs long-term depression (LTD) in L2/3 of V1, albeit at concentrations 250 times greater than the inhibitory constant (K_i) (2 micromolar vs. 8 nanomolar)⁶⁶. Twice daily injections of AM-251 prevented OD plasticity in L2/3 during 4 days of MD. However, this treatment had no detectable effect on OD plasticity in L5. Thus, OD plasticity in L5 does not require corresponding plasticity in L2/3. This finding is not consistent with OD plasticity relying on a canonical cortical microcircuit. We propose that L2/3 and L5 operate more independently than expected from the canonical circuit model.

Recent work has identified that some thalamic neurons receive binocular input and display OD plasticity^{67–69}. One calcium imaging study estimated that 15% of LGN neurons are binocular in the adult mouse⁶⁸. A second study similar in design reported 6% of neurons have binocular responses⁷⁰. However, multi-unit recordings from linear electrode arrays positioned in LGN reveal that OD shifts in V1 are largely not inherited from thalamus⁶⁹. Our experiments do not discriminate whether the OD shifts we observe in L4 with 2 days of MD in WT mice are a result of OD plasticity

by L4 neurons, or a consequence of plasticity within LGN that is then inherited by L4, or some combination of both. But given that deletion of *ngr1* in L4 but not LGN is sufficient to permit OD plasticity in adult mice, we favor the model that L4 gates OD plasticity. Likewise, the thalamocortical, intracortical, and callosal contributions to OD plasticity in L2/3 and L5 remain unclear⁷¹. Future work will be required to investigate these possible circuit mechanisms for experience-dependent visual plasticity.

The mouse has limitations for understanding visual system circuitry but has proven a useful model for investigating tuning characteristics of neurons in visual cortex that conserved with other mammals⁷², as well as experience-dependent plasticity⁸. Here we have exploited genetic resources for the mouse in combination with electrophysiology and circuit manipulations to probe how experience-dependent plasticity is coordinated within the laminar circuitry of V1. We conclude from these experiments that L4 regulates intracortical disinhibition to gate OD plasticity in visual cortex and that OD plasticity advances faster in L4 than L2/3 or L5 but does not rely on a canonical cortical microcircuit for expression.

CHAPTER III

TROY AND LINGO ARE NOT CO-RECEPTORS THAT TRANSDUCE SIGNAL BY NGR1 TO LIMIT VISUAL PLASTICITY

Introduction

NGR1 is required to close the critical period yet how it limits visual plasticity remains a challenge. NGR1 lacks a transmembrane domain and is attached to the outer leaflet of the plasma membrane by a glycosylphosphatidylinositol (GPI) anchor⁷³. The NGR1 protein contains multiple leucine-rich repeat (LRR) domains. Several proteins containing LRR domains have been implicated as regulators of synaptogenesis and plasticity, such as the LRR transmembrane neuronal protein (LRRTM) family⁷⁴. However, the cellular mechanism by which NGR1 functions is poorly understood.

Based on binding experiments *in vitro*, NGR1 is proposed to signal through one or more distinct transmembrane 'co-receptors' including TROY, Lingo-1, PlexinA2, and P75NTR⁷⁵⁻⁷⁸. NGR1 is reported to form a signaling complex with LRR and immunoglobulin domain-containing nogo receptor interacting protein (Lingo-1) and tumor necrosis factor receptor 10 (TROY)^{75,76}. Support for these proteins as co-receptors derives from experiments in which neutralizing signaling by TROY in cultured dorsal root ganglion neurons alleviates the inhibition of neurite outgrowth by myelin-associated inhibitors (MAIs) *in vitro*^{75,78}. Lingo-1 is proposed to serve as an adaptor in the signaling complex. When NGR1 binds MAIs in the presence of TROY and Lingo-1, it is reported that the intracellular signaling molecule RhoA is activated to transduce an inhibitory signal⁷⁶.

NGR1 is also reported to form a ternary complex with PlexinA2 and collapsin response mediator protein 2 (CRMP2)⁷⁷. Support for PlexinA2 as a co-receptor derives from experiments elucidating the mechanisms by which NGR1 limits recovery after brain or spinal cord trauma. Interaction of Nogo-A, a ligand of NGR1, with NGR1 limits regenerative axonal sprouting and

functional recovery after traumatic injury. CRMP2, a cytosolic protein implicated in axon growth inhibition, associates with NGR1 after NGR1 and Nogo-A interact. The Nogo-A-induced association of NGR1 and CRMP2 requires PlexinA2 as a co-receptor⁷⁷. This NGR1/PlexinA2/CRMP2 ternary complex limits neural repair after CNS trauma.

TROY and p75NTR are proposed to be functional homologs though they share modest conservation of their primary amino acid sequence. Although it has been reported that genetic deletion of p75NTR alleviates the inhibition of neurite outgrowth *in vitro*, a more recent paper has reported that deleting P75NTR in PV(+) interneurons does not promote sensitivity to brief MD after the critical period^{78,79}.

These transmembrane proteins have little similarity in their primary amino acid homology or organization of protein binding domains (data not shown). Furthermore, it is unclear whether these studies *in vitro* have physiological relevance. It is unknown which, if any, of these co-receptors transduces the signal from NGR1 to limit any facet of visual plasticity (Figure 3-1). Each potential co-receptor is expressed in visual cortex and/or thalamus⁷⁹⁻⁸¹.

Methods

Monocular Deprivation (MD)

One eye was closed on P27 or 28 (P27/8) using a single mattress suture tied with 6-0 polypropylene monofilament (Prolene 8709H; Ethicon) under brief isoflurane anesthesia (1.5 - 2%). The knot was sealed with cyanoacrylate glue. The suture was removed 4 days later under isoflurane anesthesia immediately prior to electrophysiologic recordings. The eye was examined under a stereomicroscope and animals with scarring of the cornea were eliminated from the study.

Long-term Monocular Deprivation (LTMD)

One eye was closed on P24 (P22-P23) using a single mattress suture tied with 6-0 polypropylene monofilament (Prolene 8709H; Ethicon) under brief isoflurane anesthesia (1.5 - 2%). The knot was sealed with cyanoacrylate glue. The suture was removed 4 weeks later at ~P50 with fine iridectomy scissors and the eyes were flushed with sterile saline. The eye was examined under

a stereomicroscope and animals with scarring of the cornea were eliminated from the study. Following eye-opening, mice received a 6-to-8-week period of binocular vision prior to the visual water task.

Visual Water Task

Visual acuity was estimated with the Visual Water Task which was executed by my colleague, Cecilia Attaway^{12,82,83}. In brief, two monitors were positioned at the wide end of a trapezoidal tank behind clear plexiglass. One monitor displayed a sinusoidal spatial frequency grating at 95% contrast, while the other displayed an isoluminant grey screen. The luminance of the two monitors was matched and gamma corrected with computer software (Eye-One Match 3). Inside the tank, the monitors were separated by a 46cm divider. The spatial frequency was determined relative to the length of this divider. The tank was filled with water and a hidden platform submerged below the surface of the water in front of the monitor displaying the grating.

Using a low spatial frequency (0.1 cycles per degree (cpd)), mice were trained to swim towards the monitor displaying the grating and hidden platform after a molding phase during which mice gradually learned to swim from a release chute at the back of the tank towards the monitors. During the training phase, when a mouse chose incorrectly, it repeated the trial on the same side until it chose correctly and was and then returned to its home cage. For both the training, and the subsequent testing phase, mice swam blocks of 10 interleaved trials in groups of 5 for a maximum of 4 blocks of trials per day.

During the testing phase, the spatial frequency was increased in small, sequential increments until an animal consistently fell to 70% accuracy. Starting at 0.1 cpd, mice had to succeed at three consecutive trials before proceeding to the next spatial frequency, which presented one more complete cycle of the sinusoidal grating. Following the first failure, mice were required to achieve 5 correct trials in a row, or 8 correct trials out of 10 at each spatial frequency before proceeding to the next higher frequency. Once a mouse failed to complete 8 correct trials out of 10 at a given spatial frequency, it was briefly retrained at half that spatial frequency to eliminate any potential 'side bias'. Then, testing resumed at the spatial frequency below the original

failure. The threshold for visual acuity was established once a mouse exhibited a consistent pattern of performance. Acuity thresholds were estimated as the spatial frequency average from three or more failures at adjacent spatial frequencies. Throughout the testing phase, any mouse that failed to find the hidden platform on the first try repeated the trial one more time before it was returned to its home cage, whether or not it chose correctly the second time.

Electrophysiological Recordings in Visual Cortex

Recordings and analysis were performed blind to genotype or drug treatment. Methods were adapted from previously published methods⁵⁶. In brief, mice were anesthetized with isoflurane (4% induction, 1-2% maintenance in O₂ during surgery). The mouse was placed in a stereotaxic frame and body temperature was maintained at 37°C by a homeostatically-regulated heat pad (TCAT-2LV, Physitemp). Dexamethasone (4 mg/kg s.c.; American Reagent) was administered to reduce cerebral edema. The eyes were flushed with saline and the corneas were protected thereafter by covering the eyes throughout the surgical procedure with ophthalmic ointment (Puralube, Dechra Pharmaceuticals), and with frequent application of saline. A craniotomy was made over visual cortex in the left hemisphere and a custom-designed aluminum head bar was attached with cyanoacrylate glue or Metabond over the right hemisphere to immobilize the animal during recording. Prior to transfer to the recording setup, a dose of chlorprothixene (0.5 mg/kg i.p.; C1761, Sigma) was administered to decrease the level of isoflurane required to maintain anesthesia to 0.6%.

Recordings were made with Epoxylite-coated tungsten microelectrodes with tip resistances of 10-15 M Ω (FHC). The signal was amplified (model 3600; A-M Systems), low-pass filtered at 3000Hz, high-pass filtered at 300Hz, and digitized (micro1401; Cambridge Electronic Design). Multi-unit activity was recorded from four to six locations separated by >90 μ m in depth for each electrode penetration. In each mouse, there were four to six penetrations separated by at least 200 μ m across the binocular region of primary visual cortex, defined by a receptive field azimuth < 25°. Responses were driven by drifting sinusoidal gratings (0.1cpd, 95% contrast), presented in six orientations separated by 30° (custom software, MATLAB). The gratings were presented for 1s of

each 3s trial. The grating was presented in each orientation in a pseudorandom order at least four times, interleaved randomly by a blank, which preceded each orientation once. Action potentials (APs) were identified in recorded traces with Spike2 (Cambridge Electronic Design). Only waveforms extending beyond 4 standard deviations above the average noise were included in subsequent analysis. For each unit, the number of APs in response to the grating stimuli was summed and averaged over the number of presentations. If the average number of APs for the grating stimuli was not greater than 50% above the blank, the unit was discarded. Units were classified as L2/3, L4, or L5 according to recording depth of the electrode measured from the pial surface. Units recorded between 150-300 microns were classified as L2/3, between 350-450 microns as L4, and between 500-700 microns as L5⁵⁷.

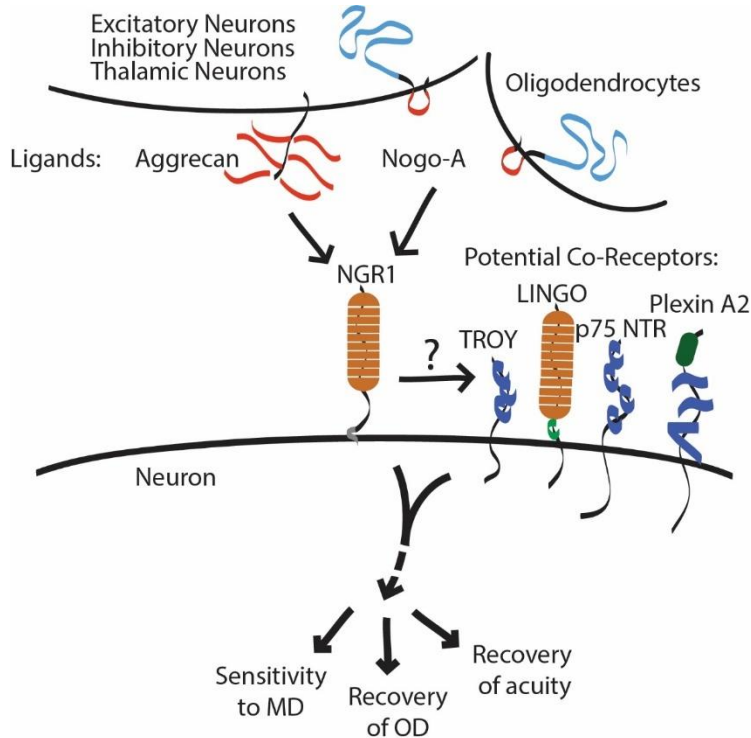
The ODI was calculated for each unit by comparing the number of APs elicited in a given unit when showing the same visual stimulus to each eye independently. Units were assigned to one of seven OD categories (1-7) where units assigned to category 1 are largely dominated by input from the contralateral eye, and units assigned to category 7 are largely dominated by input from the ipsilateral eye¹³. To categorize each unit, the average number of APs elicited by the blank was subtracted from the average number of APs elicited by the gratings for the contralateral eye (CE) and the ipsilateral eye (IE). Next, the ODI, given by $ODI = (IE - CE)/(IE + CE)$ was calculated for each unit and assigned to OD categories 1-7 as follows: -1 to -0.6 = 1, -0.6 to -0.4 = 2, -0.4 to -0.1 = 3, -0.1 to 0.1 = 4, 0.1 to 0.4 = 5, 0.4 to 0.6 = 6, 0.6 to 1 = 7. Finally, the sum of the number of cells in each category was used to calculate the CBI for each animal with the formula: $CBI = [(n1 - n7) + (2/3)(n2 - n6) + (1/3)(n3 - n5) + N]/2N$ where N is the total number of units and n_x is the number of units with OD scores equal to x ¹⁹.

Results

If any of these putative co-receptors transduces the signal from NGR1 to limit recovery of acuity following LTMD, the sensitivity to brief MD, or recovery of OD following LTMD, then mutant mice lacking this co-receptor should phenocopy the recovery of visual function following LTMD and sustained sensitivity to MD evident in constitutive *ngr1* mutant mice^{46,47}. We examined the

requirement for two putative co-receptors, TROY and LINGO, in transducing the signal from NGR1 to limit plasticity in visual circuitry (Figure 3-1).

Figure 3-1. A schematic of the ligands and co-receptors for NGR1. The ligands aggrecan and nogo are expressed by cortical excitatory and inhibitory neurons, as well as thalamic neurons. Nogo is also expressed by oligodendrocytes. NGR1 may transduce a signal through one or more co-receptors. Which co-receptors are required to close the critical period for sensitivity to monocular deprivation, recovery of OD after LTMD, and recovery of acuity after LTMD are unknown. Colored shapes in the schematic correspond to different protein binding domains.



First, we examined whether TROY or LINGO are involved in signaling by NGR1 to limit the recovery of acuity following LTMD during the critical period. We occluded one eye by lid suture in TROY mutant mice (*troy* ^{-/-}), LINGO mutant mice (*lingo* ^{-/-}) and TROY/LINGO double mutant mice (*troy* ^{-/-}; *lingo* ^{-/-}) from P22-P50 (4 weeks) spanning the critical period for sensitivity of acuity to visual experience and then removed the lid suture to provide mice with binocular vision for 8 or more weeks¹². WT mice display a persistent deficit in visual acuity through the affected eye following this LTMD¹². Acuity for WT mice is typically in the range of 0.25 to 0.35 cpd. In contrast, mice lacking a functional gene for *ngr1* exhibit substantial recovery of acuity, often with acuity indistinguishable from WT mice in the range of 0.40 to 0.50 cpd⁴⁷. TROY constitutive mutant mice (*troy* ^{-/-}), LINGO mutant constitutive mice (*lingo* ^{-/-}) and TROY/LINGO double mutant mice (*troy* ^{-/-}; *lingo* ^{-/-}), all possess low acuity after LTMD similar to WT mice (Figure 3-2). Thus, we find no

evidence that either TROY or LINGO are involved in the signal transduction by NGR1 to limit the recovery of acuity following LTMD.

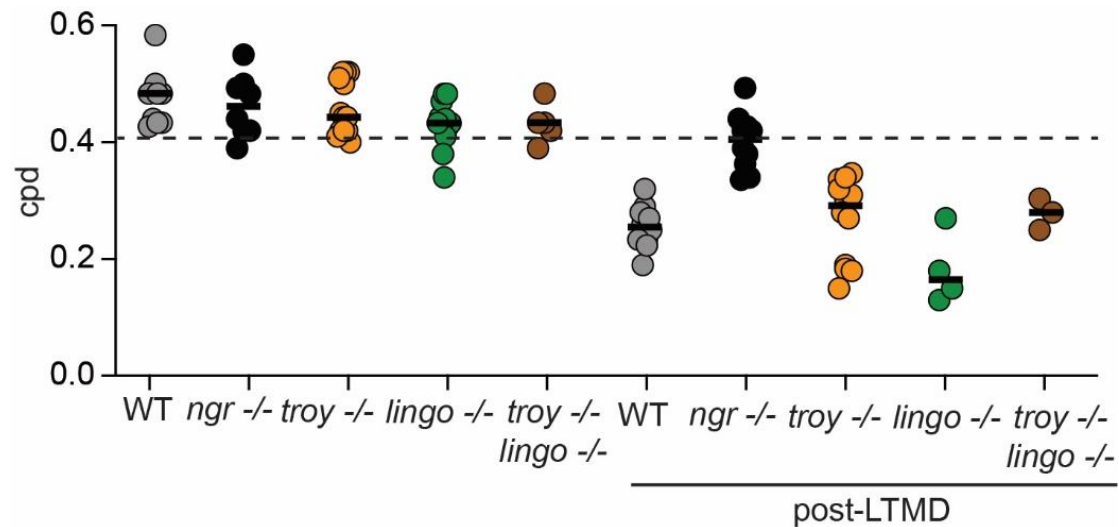


Figure 3-2. *Troy*^{-/-} mice, *lingo*^{-/-} mice, and *troy*^{-/-}; *lingo*^{-/-} do not phenocopy the recovery of acuity observed in *ngr1*^{-/-} mice after LTMD. Visual acuity of non-deprived adult mice and after 7 weeks of binocular vision following LTMD for the following genotypes: WT (grey, n=10, 10), *ngr1*^{-/-} (black, n=8,10), *troy*^{-/-} (orange, n=13, 12), *lingo*^{-/-} (green, n=12, 4), *troy*^{-/-}; *lingo*^{-/-} (brown, n=5,3). All non-deprived mice have similar acuity. Only *ngr1*^{-/-} mice recover acuity to near normal levels post-LTMD. (*ngr1* mice were originally reported in Stephany et al. 2018).

Next, we tested whether *troy*^{-/-} mice and *troy*^{-/-}; *lingo*^{-/-} mice exhibit sensitivity to brief MD as adults. One study has reported that deleting P75NTR in PV(+) interneurons does not promote sensitivity to brief MD after the critical period⁷⁹. We evaluated OD plasticity in adult *troy*^{-/-} and *troy*^{-/-}; *lingo*^{-/-} mice following 4 days of MD (P60-90). These mice did not display OD plasticity as adults as their CBI scores that were indistinguishable from WT mice and non-deprived littermate controls (Figure 3-3).

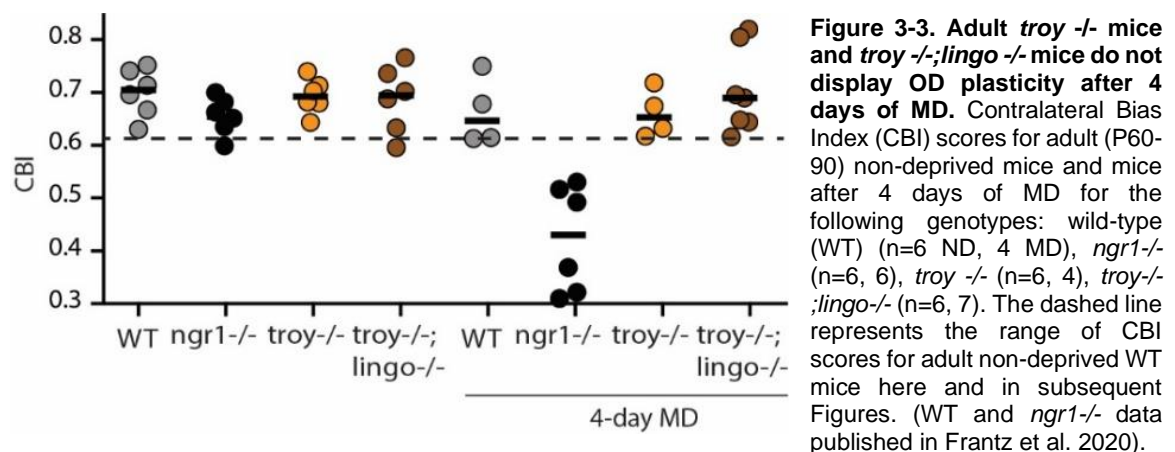


Figure 3-3. Adult *troy*^{-/-} mice and *troy*^{-/-}; *lingo*^{-/-} mice do not display OD plasticity after 4 days of MD. Contralateral Bias Index (CBI) scores for adult (P60-90) non-deprived mice and mice after 4 days of MD for the following genotypes: wild-type (WT) (n=6 ND, 4 MD), *ngr1*^{-/-} (n=6, 6), *troy*^{-/-} (n=6, 4), *troy*^{-/-}; *lingo*^{-/-} (n=6, 7). The dashed line represents the range of CBI scores for adult non-deprived WT mice here and in subsequent Figures. (WT and *ngr1*^{-/-} data published in Frantz et al. 2020).

Deletion of *ngr1* from only layer 4 neurons is sufficient to sustain sensitivity to brief MD in adult mice⁶². In comparison, deletion of *ngr1* from all excitatory neurons in forebrain is required to permit recovery of normal eye dominance following LTMD⁵⁶. Thus, retaining OD plasticity for brief MD relies on different mechanisms than OD plasticity for recovery from LTMD; OD plasticity for brief MD relies on a subset of neurons relative to OD plasticity for recovery of normal OD following LTMD. Given that constitutive deletion of TROY and LINGO in all neurons did not improve recovery of acuity or sensitivity to brief MD, we did not examine recovery of OD following LTMD.

Discussion

Other than TROY and LINGO, alternative putative co-receptors mentioned above may be involved in future research to understand the cellular mechanisms of NGR1. However, a recent paper has published that deleting P75NTR in PV(+) interneurons does not promote sensitivity to brief MD after the critical period⁷⁹. On the contrary, PlexinA2 may be a viable candidate for the co-receptor that transduces the signal by NGR1 to limit plasticity. Research has suggested that an NGR1/PlexinA2/CRMP2 ternary complex limits neural repair after CNS trauma. The Nogo-A-induced association of NGR1 and CRMP2 requires PlexinA2 as a co-receptor, suggesting an indirect role for PlexinA2 in limiting plasticity⁷⁷. Future work may focus on PlexinA2 as the transducing co-receptor as well as the resulting complex between NGR1 and CRMP2 as a mechanism by which NGR1 limits plasticity. Overall, I conclude that TROY and LINGO are not co-receptors that transduce the signal by NGR1 to limit visual plasticity.

CHAPTER IV
PERINEURONAL NETS ARE NOT REQUIRED
TO CLOSE THE CRITICAL PERIOD FOR OD PLASTICITY

Introduction

Several chondroitin sulfate proteoglycans (CSPGs) are concentrated in PNNs^{84,85}. These molecules comprise a peptide backbone decorated with chondroitin sulfate glycosaminoglycans (CS-GAGs). CSPGs are typically large molecules with a protein core that is more than 100 kilodaltons (kDa) and apparent molecular weights that often exceed several hundred kDa due to the chains of CS-GAGs. A consequence of the large size and complexity of these molecules is that their diverse functions are poorly understood^{86–88}. Interestingly, PNNs surround parvalbumin-positive (PV) interneurons^{89,90}. The principal CSPG aggrecan is expressed by both excitatory and inhibitory neurons, and is present in nearly all (>96%) PNNs^{85,89,90}.

There are several lines of evidence associating PNNs and aggrecan in the closure of the critical period. First, the number of PNNs and the staining intensity for the CSPG aggrecan in primary visual cortex (V1) correlates with the closure of the critical period during both normal development and with dark-rearing that delays the critical period^{90–92}. Second, adult rats treated with the enzyme chondroitinase ABC (chABC) that degrades CS-GAGs, dermatin sulfate, and hyaluronan GAGs, exhibit partial recovery of sensitivity to brief MD, as well as recovery of normal eye dominance and acuity following LTMD when combined with ‘reverse suture’ of the non-deprived eye^{43,44,93,94}. Third, mice in which *acan* has been selectively deleted in neuronal and glial precursors throughout the central nervous system display OD plasticity after the critical period^{95,96}. Last, NGR1 is also a high affinity receptor for the chondroitin sulfate glycosaminoglycan (CS-GAG) moiety of CSPGs (Figure 3-1)¹⁸. However, these studies indirectly implicate PNNs as factors closing the critical period because they are unable to discriminate whether this enhanced adult

visual plasticity is a consequence of loss of PNNs, or the loss of aggrecan expression elsewhere in the neuropil outside of PNNs.

Genetic studies of the role of aggrecan in restricting visual plasticity are hindered by the fact that the *acan* constitutive mutant is embryonic lethal, likely because of impaired cartilage formation in essential structures such as the trachea^{97,98}. Deleting *acan* in neuronal and glial precursors throughout the central nervous system with *Nestin-Cre* abolishes PNNs and also enhances OD plasticity in adult mice as measured with optical imaging of intrinsic signals⁹⁵. However, which neurons express *acan* to abolish PNNs, and how this relates to the role of *acan* in limiting OD plasticity remains unknown.

Methods

Mice

The conditional *acan flx/flx* mouse strains has been characterized⁹⁵. This strain was rederived at Jackson laboratories and subsequently crossed to the *PV-Cre*, *DLX5a-Cre*, *GAD2-Cre* and *BAF53-Cre* Cre driver lines obtained from Jackson labs (strain numbers 008069, 008199, 028867, and 027826, respectively). The specificity for each Cre driver line was validated by crossing each line to the Cre reported line *Ai14* (tdTomato) (The Jackson Laboratory, strain 007914). Experiments and procedures were performed on both adult male and female mice blind to genotype and/or treatment condition. Mice were group housed and maintained on a 12-hr light/dark cycle under standard housing conditions. For experimental and control groups including the *acan flx/flx* line, experiments were performed on littermates. Genotyping was performed using custom primer sets for polymerase chain reaction (PCR) amplification with REDExtract-N-Amp PCR kit (XNAT, Sigma).

Immunohistochemistry

Mice were deeply anesthetized with Ketamine HCl (200mg/Kg, Phoenix pharmaceuticals)/Xylazine (20mg/Kg, Lloyd Laboratories) and transcardially perfused with phosphate buffered saline (PBS) (Sigma-Aldrich, D1408) followed by a buffered 4%

paraformaldehyde (PFA)/PBS (Acros Organics 416780030). Brains post-fixed overnight in 4% PFA/PBS. Free-floating 40-micron sections were cut on a vibrating microtome (Leica VT 1000S) and preserved in PBS containing 0.05% sodium azide (Sigma-Aldrich S8032).

Coronal sections containing visual cortex were washed in Tris-Buffered Saline (TBS, 50mM Tris-HCl, 150mM NaCl, pH 7.4) (3 X 5 minutes) and then incubated in 100mM sodium citrate buffer pH 4.5 (Sigma-Aldrich S1804) at 95°C for 10 minutes for antigen retrieval. Sections were allowed to cool to room temperature and then washed in TBS (3 X 10 minutes). Sections were incubated in blocking solution, 3% normal horse serum (NHS; Vector Laboratories S-2000) in PBS containing 0.3% Triton X-100 (Sigma-Aldrich T9284) for 1 hour at room temperature (TBS-T).

In sections labeled for PNNs, fluorescein conjugated Wisteria Floribunda Agglutinin (WFA) (VectorLabs, FL-1351) was diluted in blocking solution to 2mg/mL. Sections incubated for an hour or longer at RT. After repeated washing in TBS-T (3 X 10 min), sections were mounted onto SuperFrost Plus slides (Fisher) with Fluoromount G containing 4',6-diamidino-2-phenylindole (DAPI) (Electron Microscopy Science).

The primary antibody rabbit anti-aggrecan (Sigma, AB1031) was diluted in blocking solution to 1mg/mL. Sections incubated for an hour or longer at RT. After repeated washing in TBS-T (3 X 10 min), sections were incubated in secondary antibody, Alexa 488-conjugated donkey anti-rabbit (Jackson Immuno Research) 1:200 in blocking solution, for 1 hour at room temperature. After a final series of washes (3x 10 min in TBS-T, 1 X 10 min in TBS), sections were mounted onto SuperFrost Plus slides (Fisher) with Fluoromount G containing 4',6-diamidino-2-phenylindole (DAPI) (Electron Microscopy Science).

Monocular Deprivation (MD)

One eye was closed on P25-27, or P60-90 using a single mattress suture tied with 6-0 polypropylene monofilament (Prolene 8709H; Ethicon) under brief isoflurane anesthesia (2%) for durations described. The knot was sealed with cyanoacrylate glue. Upon removing the suture, the eye was examined under a stereomicroscope and animals with scarring of the cornea were eliminated from the study.

Visual Water Task

Visual acuity was estimated with the Visual Water Task^{12,82,83}. In brief, two monitors were positioned at the wide end of a trapezoidal tank behind clear plexiglass. One monitor displayed a sinusoidal spatial frequency grating at 95% contrast, while the other displayed an isoluminant grey screen. The luminance of the two monitors was matched and gamma corrected with computer software (Eye-One Match 3). Inside the tank, the monitors were separated by a 46cm divider. The spatial frequency was determined relative to the length of this divider. The tank was filled with water and a hidden platform submerged below the surface of the water in front of the monitor displaying the grating.

Using a low spatial frequency (0.1 cycles per degree (cpd)), mice were trained to swim towards the monitor displaying the grating and hidden platform after a molding phase during which mice gradually learned to swim from a release chute at the back of the tank towards the monitors. During the training phase, when a mouse chose incorrectly, it repeated the trial on the same side until it chose correctly and was and then returned to its home cage. For both the training, and the subsequent testing phase, mice swam blocks of 10 interleaved trials in groups of 5 for a maximum of 4 blocks of trials per day.

During the testing phase, the spatial frequency was increased in small, sequential increments until an animal consistently fell to 70% accuracy. Starting at 0.1 cpd, mice had to succeed at three consecutive trials before proceeding to the next spatial frequency, which presented one more complete cycle of the sinusoidal grating. Following the first failure, mice were required to achieve 5 correct trials in a row, or 8 correct trials out of 10 at each spatial frequency before proceeding to the next higher frequency. Once a mouse failed to complete 8 correct trials out of 10 at a given spatial frequency, it was briefly retrained at half that spatial frequency to eliminate any potential 'side bias'. Then, testing resumed at the spatial frequency below the original failure. The threshold for visual acuity was established once a mouse exhibited a consistent pattern of performance. Acuity thresholds were estimated as the spatial frequency average from three or more failures at adjacent spatial frequencies. Throughout the testing phase, any mouse that failed

to find the hidden platform on the first try repeated the trial one more time before it was returned to its home cage, whether or not it chose correctly the second time.

Electrophysiological Recordings in Visual Cortex

Recordings and analysis were performed blind to genotype or drug treatment. Methods were adapted from previously published methods⁵⁶. In brief, mice were anesthetized with isoflurane (4% induction, 1-2% maintenance in O₂ during surgery). The mouse was placed in a stereotaxic frame and body temperature was maintained at 37°C by a homeostatically-regulated heat pad (TCAT-2LV, Physitemp). Dexamethasone (4 mg/kg s.c.; American Reagent) was administered to reduce cerebral edema. The eyes were flushed with saline and the corneas were protected thereafter by covering the eyes throughout the surgical procedure with ophthalmic ointment (Puralube, Dechra Pharmaceuticals), and with frequent application of saline. A craniotomy was made over visual cortex in the left hemisphere and a custom-designed aluminum head bar was attached with cyanoacrylate glue or Metabond over the right hemisphere to immobilize the animal during recording. Prior to transfer to the recording setup, a dose of chlorprothixene (0.5 mg/kg i.p.; C1761, Sigma) was administered to decrease the level of isoflurane required to maintain anesthesia to 0.6%.

Recordings were made with Epoxylite-coated tungsten microelectrodes with tip resistances of 10-15 M Ω (FHC). The signal was amplified (model 3600; A-M Systems), low-pass filtered at 3000Hz, high-pass filtered at 300Hz, and digitized (micro1401; Cambridge Electronic Design). Multi-unit activity was recorded from four to six locations separated by >90 μ m in depth for each electrode penetration. In each mouse, there were four to six penetrations separated by at least 200 μ m across the binocular region of primary visual cortex, defined by a receptive field azimuth < 25°. Responses were driven by drifting sinusoidal gratings (0.1cpd, 95% contrast), presented in six orientations separated by 30° (custom software, MATLAB). The gratings were presented for 1s of each 3s trial. The grating was presented in each orientation in a pseudorandom order at least four times, interleaved randomly by a blank, which preceded each orientation once. Action potentials (APs) were identified in recorded traces with Spike2 (Cambridge Electronic Design). Only

waveforms extending beyond 4 standard deviations above the average noise were included in subsequent analysis. For each unit, the number of APs in response to the grating stimuli was summed and averaged over the number of presentations. If the average number of APs for the grating stimuli was not greater than 50% above the blank, the unit was discarded. Units were classified as L2/3, L4, or L5 according to recording depth of the electrode measured from the pial surface. Units recorded between 150-300 microns were classified as L2/3, between 350-450 microns as L4, and between 500-700 microns as L5⁵⁷.

The ODI was calculated for each unit by comparing the number of APs elicited in a given unit when showing the same visual stimulus to each eye independently. Units were assigned to one of seven OD categories (1-7) where units assigned to category 1 are largely dominated by input from the contralateral eye, and units assigned to category 7 are largely dominated by input from the ipsilateral eye¹³. To categorize each unit, the average number of APs elicited by the blank was subtracted from the average number of APs elicited by the gratings for the contralateral eye (CE) and the ipsilateral eye (IE). Next, the ODI, given by $ODI = (IE - CE)/(IE + CE)$ was calculated for each unit and assigned to OD categories 1-7 as follows: -1 to -0.6 = 1, -0.6 to -0.4 = 2, -0.4 to -0.1 = 3, -0.1 to 0.1 = 4, 0.1 to 0.4 = 5, 0.4 to 0.6 = 6, 0.6 to 1 = 7. Finally, the sum of the number of cells in each category was used to calculate the CBI for each animal with the formula: $CBI = [(n1 - n7) + (2/3)(n2 - n6) + (1/3)(n3 - n5) + N]/2N$ where N is the total number of units and n_x is the number of units with OD scores equal to x ¹⁹.

Quantification and Statistical Analysis

All statistical analyses were performed using Prism software (version 8.0, GraphPad). Group numbers are stated in the Results and Figure Legends. N represents the number of mice for group comparisons and units for cumulative distributions, except for Figures 4 and 5 where n corresponds to the number of cells. Unless otherwise stated, group comparisons were made using the Kruskal-Wallis test with Dunn's correction. The specific pairwise tests are described in the Results section. Values presented are the mean plus/minus the standard deviation.

Results

Single-cell expression data indicates that *acan* is predominantly expressed by PV interneurons with only trace expression in other neurons cell types and astrocytes⁹⁹. Given that PNNs surround PV interneurons in V1³¹, and injection of chABC into V1 promotes visual plasticity⁴³, we focused our genetic dissection of the requirement of *acan* expression to confine OD plasticity to the critical period on PV interneurons and expanded to larger populations of neurons overlapping with PV interneurons. First, we generated homozygous *acan flx/flx*; *PV-Cre* mice¹⁰⁰. Then we generated two more lines with Cre recombinase expression in a larger population of interneurons that include PV interneurons: *Dlx5a-Cre* and *GAD2-Cre*. *Dlx5a-Cre* is expressed by cells migrating from the ganglionic eminence and labels inhibitory neurons in the forebrain and other brain regions¹⁰¹. *GAD2-Cre* is expressed by all GABA-positive inhibitory neurons in the brain¹⁰². In addition, we combined *acan flx* with *BAF53-Cre*, a pan-neuronal driver¹⁰³.

PNNs are readily detected in the neuropil by staining with fluorescently labeled wisteria floribunda agglutinin (WFA)^{104,105}. This lectin binds N-acetylgalactosamine residues of CSPGs¹⁰⁴. Deleting *acan* throughout the brain with *Nestin-Cre* eliminates PNNs⁹⁵. Likewise, in contrast to *acan flx/flx* littermates, only a handful of PNNs were evident in coronal sections of visual cortex from adult *acan flx/flx*; *PV-Cre* mice (Figure 4-1). This small number of PNNs was further reduced, if not completely eliminated, in *acan flx/flx* mice in combination with *Dlx5a-Cre*, *GAD2-Cre*, or *BAF53-Cre* (Figure 4-1). Thus, *acan* expression in inhibitory neurons is required for PNNs in visual cortex.

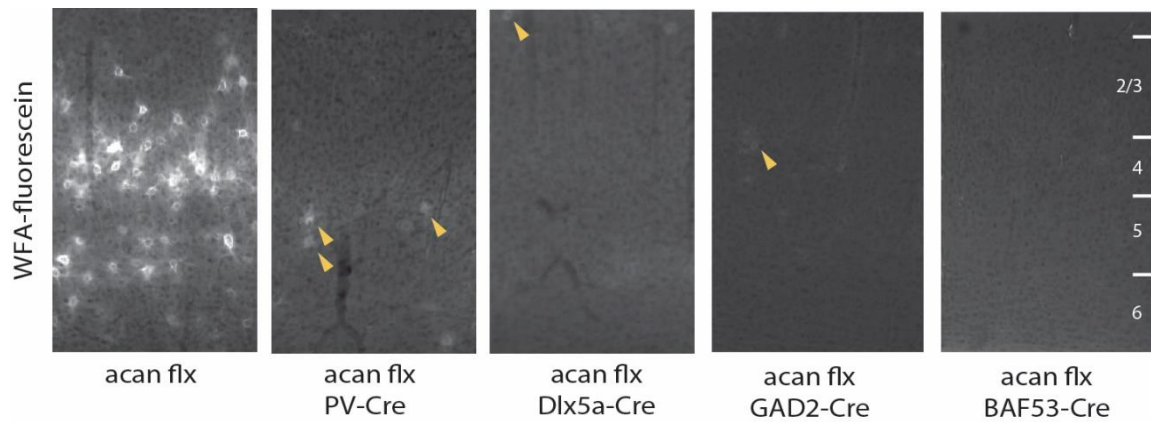


Figure 4-1. *Acan* is required in cortical inhibitory neurons for the formation of PNNs. Coronal sections of visual cortex stained with wisteria floribunda agglutinin (WFA) linked to fluorescein to label PNNs for *acan flx/flx* mice alone (*acan flx*) or in combination with *PV-Cre*, *Dlx5a-Cre*, *GAD2-Cre* or *BAF53-Cre*. Residual PNNs are indicated by yellow arrowheads. Approximate positions of cortical layers are indicated at right.

Deletion of *acan* throughout the brain with *Nestin-Cre* also disrupts the localization of several other CSPGs to PNNs including brevican, neurocan, phosphacan, and versican, as well as the hyaluronan and proteoglycan link protein-1 (HAPLN1)⁹⁵. HAPLN1 is required for the enrichment of these CSPGs in PNNs⁸⁴. To investigate the relationship between the localization of WFA staining and aggrecan, we immunostained coronal sections of visual cortex from *acan flx/flx* mice alone and in combination with each of the four Cre drivers – *PV-Cre*, *Dlx5a-Cre*, *GAD2-Cre*, and *BAF53-Cre* – with antibodies specific for aggrecan (Figure 4-2). In *acan flx/flx* mice, the signal for aggrecan was enriched around cell somas in a pattern similar to WFA staining (Figure 4-1), but also evident throughout the adjacent neuropil. In *acan flx/flx; PV-Cre* mice, only a small number of soma were surrounded by greater intensity staining for aggrecan across layers. In comparison, only a small subset of cell somas displayed signal for aggrecan in *acan flx/flx* mice in combination with *Dlx5a-Cre* and *GAD2-Cre*. These appeared predominantly in layer 5. No enrichment around cell somas was evident for *acan flx/flx; BAF53-Cre* mice. Thus, detectable aggrecan immunostaining is associated with neuronal expression.

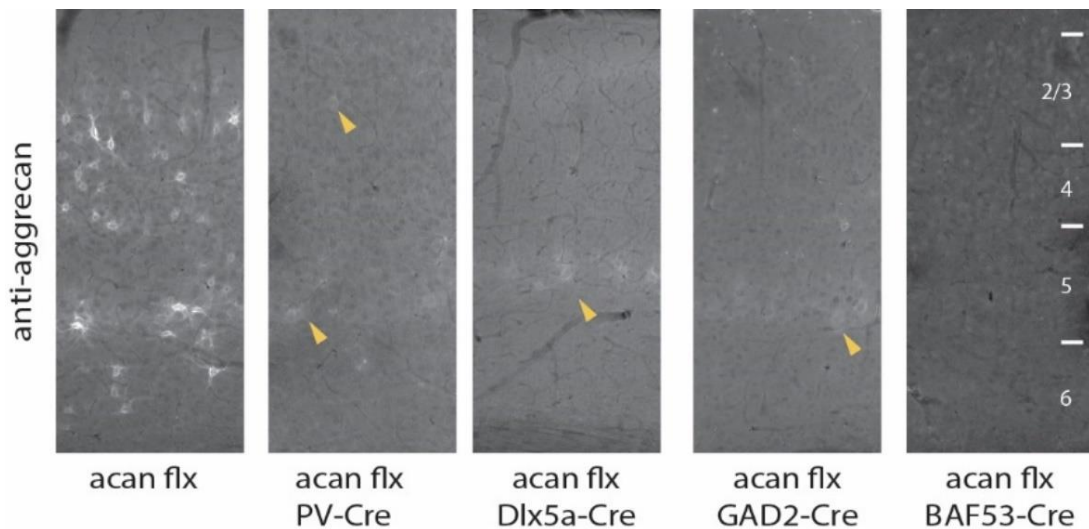
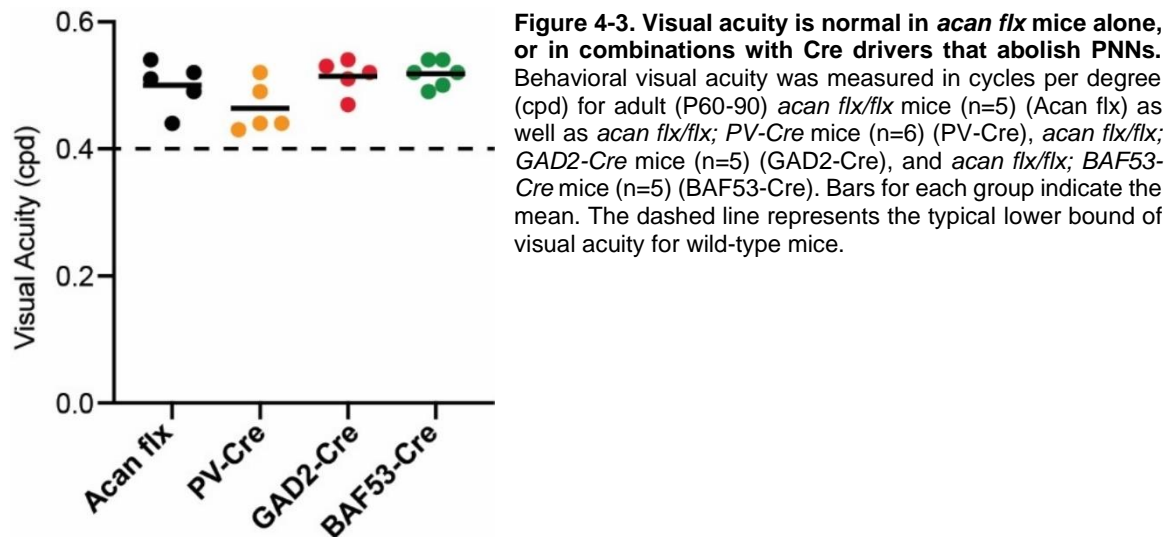


Figure 4-2. Deleting *acan* in cortical inhibitory neurons abolishes enrichment of aggrecan around cell soma except for a small population in layer 5. Coronal sections of visual cortex stained with antibodies directed against aggrecan for *acan flx/flx* mice alone (*acan flx*) or in combination with *PV-Cre*, *Dlx5a-Cre*, *GAD2-Cre* or *BAF53-Cre*. Some cell somas surrounded by aggrecan signal are observed *acan flx/flx* mice in combination with Cre drivers for inhibitory neurons (yellow arrowheads). Approximate positions of cortical layers are indicated at right.

To determine if selective deletion of *acan* and eliminating PNNs resulted in gross disruptions of visual circuitry and vision, we examined visual acuity in *acan flx/flx* mice, *acan*

flx/flx;PV-Cre mice, *acan flx/flx; GAD2-Cre* mice, and *acan flx/flx; BAF53-Cre* mice (Figure 4-3). We did not examine *acan flx/flx; Dlx5a-Cre* mice because the Cre expression directed to inhibitory neurons is very similar to that in *GAD2-Cre* mice. We measured acuity with the visual water task⁸². Adult wild-type mice typically exhibit acuity in the range of 0.5 cycles per degree (cpd) when tested with this behavioral assay⁸². This task relies on visual cortex¹⁰⁶. In contrast to our experiments measuring monocular visual acuity following LTMD (Figure 3-2), here we measured binocular visual acuity. Overall, deleting *acan* either selectively in PV neurons with *PV-Cre*, interneurons with *GAD2-Cre*, or all neurons with *BAF53-Cre*, had no effect on acuity (Figure 4-3). The mean and standard deviation for each group were indistinguishable between genotypes: *acan flx/flx* alone ($0.50 \pm .04$, $n=5$), *acan flx/flx;PV-Cre* ($0.46 \pm .04$, $n=5$), *acan flx/flx; GAD2-Cre* ($0.51 \pm .03$, $n=5$), and *acan flx/flx; BAF53-Cre* ($0.52 \pm .02$, $n=6$). The minor differences in average acuity are not significant (Kruskal-Wallis (KW) test, each genotype vs. *acan flx/flx*, $P > .53$ for each comparison).



The first studies examining visually-evoked responses in the mouse were published in the 1970s^{20,58}. These experiments revealed that MD performed at P11-12 and sustained 6 weeks to a year prior to performing electrophysiologic recordings under barbiturate anesthesia results in a shift in OD to favor the non-deprived eye²⁰. These original studies were later extended in the 1990s to determine the effects of MD for each layer in visual cortex, the duration of MD that yields saturating

shifts in OD, and the timing of the critical period¹⁹. This study established the sensitivity of the critical period to brief (4-day) MD extends from P19 to P32. These recordings were also performed under barbiturate anesthesia.

As a prelude to testing whether the critical period closes normally in mice lacking *acan* expression in overlapping populations of neurons, we first confirmed the age at which the critical period closes with our experimental preparation that employs isoflurane rather than barbiturates for anesthesia⁵⁰. We measured eye dominance with multi-unit electrophysiologic recordings for non-deprived juvenile mice (P26-P28) and adult mice (P60-90), as well as for juvenile WT mice that received MD for 4 days beginning at P28, P30, P33, P36, and P39 (Figure 4-4). Both juvenile and adult mice display contralateral bias index scores (CBI) between 0.65 and 0.75. This is the normal range of eye dominance for mice¹⁹. In contrast, mice receiving 4 days of MD beginning at P28 or P30 displays significantly lower CBI scores ($P=.001$ and $.003$, respectively, KW test corrected for 6 comparisons). However, MD started at P33 or older ages results in a much smaller shift in CBI values that are not significantly different from non-deprived juvenile mice ($P = 0.26$ and higher) (Figure 4-4). Thus, in our hands, the critical period closes around P32 as predicted from classic studies of OD plasticity in the mouse.

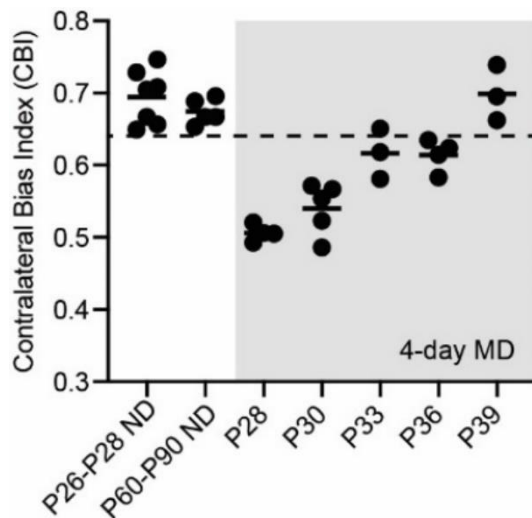
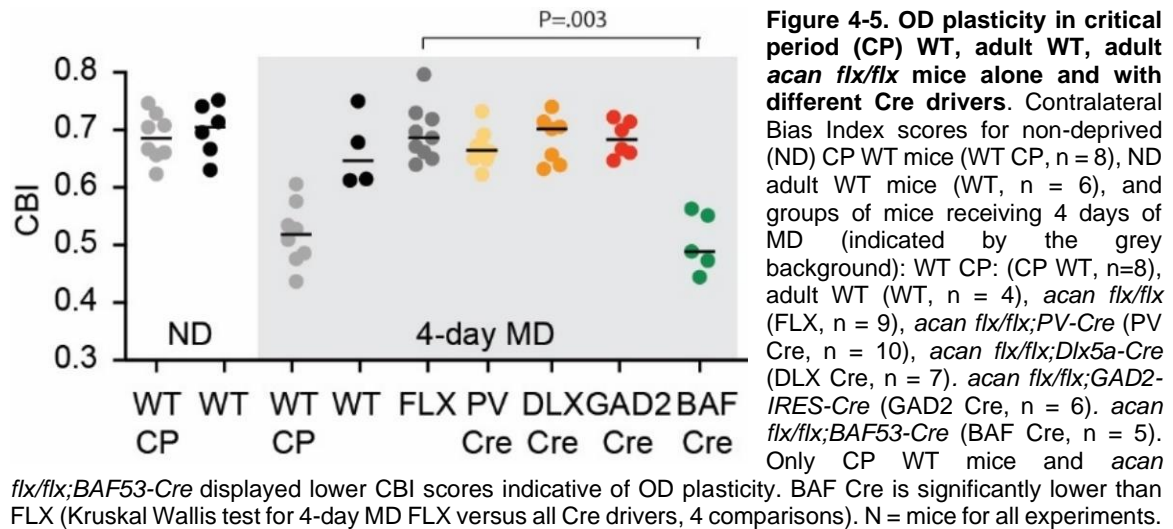


Figure 4-4. The critical period closes around P32. Average contralateral bias index (CBI) scores for different ages of mice (black circles): Critical period and adult nondeprived (ND) groups show a non-shifted CBI. P28 mice show a shifted CBI after 4 days of MD. P30, P33, and P36 mice show progressively increased CBIs after 4 days of MD. P39 mice show a non-shifted CBI, similar to ND mice. This reproduces data from Gordon and Stryker, 1996.

In preliminary experiments, adult (P60-90) *acan flx/flx* mice in combination with *PV-Cre* did not exhibit OD plasticity with 4 days of MD despite a dramatic reduction in the number of PNNs in

primary visual cortex (Figure 4-5). We were surprised that these mice did not exhibit any evident OD plasticity (*acan flx/flx* alone (FLX), CBI = 0.69, n = 9 mice); with *PV-Cre* (PV Cre, CBI = 0.67; n = 10 mice). To confirm this result, we tested OD plasticity in adult *acan flx/flx* mice with more extensive Cre recombinase in GABAergic neurons from *Dlx5a-Cre* and *GAD-IRES-Cre*. These mice also did not display OD plasticity (DLX Cre, CBI = 0.68, n = 8; GAD2 Cre, CBI = 0.68, n = 7) (Figure 4-5). We only observed OD plasticity in *acan flx/flx* in combination with *BAF53-Cre* mice, a pan-neuronal Cre driver (BAF Cre, CBI = 0.50, n = 5). Thus, the elimination of PNNs is not sufficient to prevent the critical period from closing and sustain OD plasticity in response to brief MD in adult mice.



Discussion

PNNs were first proposed as extracellular factors that close the critical period for experience-dependent visual plasticity more than 30 years ago⁹². However, discriminating whether PNNs containing aggrecan are required to close the critical period, or whether aggrecan expression within the neuropil that is not associated with PNNs limits visual plasticity, has proven elusive. Here we harnessed the genetic and molecular resources available for the mouse to overcome barriers to identify the roles of PNNs and the principal CSPG aggrecan in confining robust experience-dependent visual plasticity to critical periods.

PNNs are proposed to contribute to a number of functions through their CSPGs binding directly to receptors, axon guidance molecules, and growth factors, among others (reviewed by ¹⁰⁷).

PNNs have been proposed to regulate the electrophysiologic properties of neurons and synaptic plasticity by interacting with ion channels (reviewed by ¹⁰⁸) and the balance of excitatory to inhibitory neurotransmission (E/I balance) by modulating the activity of ensheathed inhibitory neurons¹⁰⁹. However, these roles of PNNs appear dispensable for the maturation of visual cortex as visual acuity and binocularity of naïve mice lacking PNNs in *acan flx/flx* mice in combination with *PV-Cre*, *Dlx5a-Cre*, *GAD2-Cre*, and *BAF53-Cre*, which all lack PNNs, are normal and indistinguishable from *acan flx/flx* controls or WT mice (Figures 4-3 and 4-5).

CSPGs are abundant in PNNs. As a consequence, the effects of manipulations that degrade CSPGs, for example treatment with ChABC, or prevent the crosslinking of CSPGs, for example deletion of the gene for HAPLN1, are most evident on PNNs^{43,84}. Both injecting chABC into visual cortex of adult rats and genetic deletion of HAPLN1 in the CNS are reported to abolish PNNs and promote OD plasticity after the close of the critical period^{43,84}. This enhanced visual plasticity was attributed to the loss of CSPGs localized to PNNs. Likewise, enhanced visual plasticity in *acan flx/flx;Nestin-Cre* mice has been asserted to be a result of loss of PNNs. However, CSPGs are also present throughout the neuropil outside of PNNs¹¹⁰.

In contrast, we observe with several distinct Cre drivers targeting *acan* deletion to inhibitory neurons that loss PNNs is not sufficient to sustain OD plasticity beyond the critical period, but that deletion of *acan* from all neurons with *BAF53-Cre* prevents the critical period from closing. Our interpretation from these experiments is that abolishing PNNs and aggrecan expression by inhibitory neurons is not sufficient to prevent the critical period from closing but eliminating expression of aggrecan by all neurons is sufficient to prevent the critical period from closing. These findings conflict with experiments performed on mice lacking neural expression of HAPLN1 in which partial loss of aggrecan and other CSPGs from PNNs was reported to sustain OD plasticity in adult mice⁸⁴. This study employed visually-evoked potentials (VEPs) with low impedance to measure visually-evoked responses anesthetized with urethane, whereas we perform multi-unit recordings with high impedance electrodes in mice anesthetized with isoflurane⁵⁰. These differences in methodology may contribute to these opposing outcomes.

Our experiments do not discriminate whether loss of CSPGs in PNNs is required but not sufficient to prevent the critical period from closing. In future experiments, one could test the requirement of loss of PNNs for sustaining OD plasticity after the critical period by comparing OD plasticity in adult mice lacking *acan* in inhibitory neurons (*GAD2-Cre*) versus all neurons (*BAF53-Cre*) versus excitatory neurons (*CamK2a-Cre*). If deleting *acan* only in excitatory neurons with *CamK2-Cre* permits OD plasticity in adult mice despite the presence of PNNs, similar to *acan flx/flx*; *BAF53-Cre* mice, this outcome would support the conclusion that PNNs do not contribute to the closure of the critical period. Reciprocally, if deleting *acan* only in excitatory neurons with *CamK2-Cre* does not permit OD plasticity in adult mice, similar to *acan flx/flx*; *GAD2-Cre* mice, this would support the conclusion that deletion of *acan* both in inhibitory neurons (and PNNs) and excitatory neurons contribute to the closure of the critical period.

CHAPTER V

SUMMARY AND FUTURE DIRECTIONS

Numerous studies to date support that NGR1 is involved in developmental plasticity^{11,17,46,47,56}. Notably, NGR1 limits plasticity to the critical period for both OD and visual acuity, though the mechanism through which this phenomenon occurs remains unknown. This study addressed 3 questions regarding neural circuitry within primary visual cortex related to NGR1 as well as possible molecular mechanisms through which NGR1 confines plasticity to the critical period. First, through the use of genetic resources to determine how experience-dependent plasticity propagates through primary visual cortex, I determined that OD plasticity advances faster in L4 than L2/3 or L5 but does not rely on a canonical cortical microcircuit for expression. Second, I determined that TROY and LINGO are not co-receptors that transduce the signal by NGR1 to limit plasticity. Last, I determined that loss of PNNs by deletion of *acan* in inhibitory interneurons is not sufficient to sustain OD plasticity beyond the critical period, but loss of PNNs by deletion of *acan* in all neurons prevents the critical period from closing. This study provides novel answers to long-standing questions within the field and opens new possibilities for future research.

Future work will be required to address questions that this study did not resolve. First, my experiments did not discriminate whether OD shifts observed in L4 with 2-day MD in WT mice are a result of OD plasticity by L4 neurons, or a consequence of plasticity within dLGN that is subsequently inherited by L4, or a combination of both. Similarly, the thalamocortical, intracortical, and callosal contributions to OD plasticity in L2/3 and L5 remain unknown. These future experiments may elucidate possible circuit mechanisms for experience-dependent visual plasticity and further define how NGR1 limits plasticity to the critical period. Second, my experiments did not address NGR1 co-receptors other than TROY and LINGO. The Nogo-A induced association of NGR1 and CRMP2 requires PlexinA2 as a co-receptor to limit neural repair after CNS trauma,

suggesting an indirect role for PlexinA2 in limiting plasticity. Future experiments may identify PlexinA2 as the co-receptor through which NGR1 limits critical period plasticity. Finally, my experiments did not discriminate whether loss of CSPGs in PNNs is required but not sufficient to prevent the critical period from closing. Future experiments will require the addition of a genetic line in which mice lack acan in excitatory neurons. If deleting acan only in excitatory neurons permits OD plasticity in adult mice despite the presence of PNNs, the evidence supports the conclusion that PNNs do not contribute to the closure of the critical period. If deleting acan only in excitatory neurons does not permit OD plasticity in adult mice, the evidence supports the conclusion that deletion of acan in both inhibitory neurons (and PNNs) and excitatory neurons contribute to the closure of the critical period. Altogether, these future experiments will contribute to understanding the role that NGR1 plays in limiting experience-dependent developmental plasticity to the critical period.

REFERENCES

1. Hensch, T. K. & Quinlan, E. M. Critical periods in amblyopia. *Visual neuroscience* vol. 35 E014 (2018).
2. Hubel, D. H. & Wiesel, T. N. Receptive fields, binocular interaction and functional architecture in the cat's visual cortex. *J. Physiol.* **160**, 106–154 (1962).
3. Kisilevsky, B. S. *et al.* Effects of Experience on Fetal Voice Recognition. <https://doi.org/10.1111/1467-9280.02435> **14**, 220–224 (2003).
4. Knudsen, E. I., Knudsen, P. F. & Esterly, S. D. Early auditory experience modifies sound localization in barn owls. *Nature* **295**, 238–240 (1982).
5. Knudsen, E. I., Esterly, S. D. & Knudsen, P. F. *MONAURAL OCCLUSION ALTERS SOUND LOCALIZATION DURING A SENSITIVE PERIOD IN THE BARN OWL*. *The Journal of Neuroscience Copyright © Society for Neuroscience* vol. 4 (1984).
6. Brainard, M. S. & Knudsen, E. I. Sensitive periods for visual calibration of the auditory space map in the barn owl optic tectum. *J. Neurosci.* **18**, 3929–3942 (1998).
7. Gordon, J. A. & Stryker, M. P. Experience-dependent plasticity of binocular responses in the primary visual cortex of the mouse. *J. Neurosci.* **16**, 3274–3286 (1996).
8. Priebe, N. J. & McGehee, A. W. Mouse vision as a gateway for understanding how experience shapes neural circuits. *Front. Neural Circuits* **8**, 1–9 (2014).
9. Antonini, A., Stryker, M. P. & Keck, W. M. *Development of Individual Geniculocortical Arbors in Cat Striate Cortex and Effects of Binocular Impulse Blockade. The Journal of Neuroscience* vol. 73 (1993).
10. Antonini, A., Fagiolini, M. & Stryker, M. P. Anatomical correlates of functional plasticity in mouse visual cortex. *J. Neurosci.* **19**, 4388–4406 (1999).
11. Stephany, C. É. C.-E., Frantz, M. G. M. G. & McGehee, A. W. A. W. Multiple Roles for Nogo Receptor 1 in Visual System Plasticity. *Neuroscientist* **22**, 653–666 (2016).

12. Prusky, G. T. & Douglas, R. M. Developmental plasticity of mouse visual acuity. *Eur. J. Neurosci.* **17**, 167–173 (2003).
13. Wiesel, T. N. & Hubel, D. H. Single-Cell Responses in Striate Cortex of Kittens Deprived of Vision in One Eye. *J. Neurophysiol.* **26**, 1003–1017 (1963).
14. Kirkby, L. A., Sack, G. S., Firl, A. & Feller, M. B. A role for correlated spontaneous activity in the assembly of neural circuits. *Neuron* **80**, 1129 (2013).
15. Sato, M. & Stryker, M. P. Distinctive features of adult ocular dominance plasticity. *J. Neurosci.* **28**, 10278–10286 (2008).
16. Baldwin, K. T. & Giger, R. J. Insights into the physiological role of CNS regeneration inhibitors. *Front. Mol. Neurosci.* **8**, 1–8 (2015).
17. McGee, A. W. & Strittmatter, S. M. The Nogo-66 receptor: focusing myelin inhibition of axon regeneration. *Trends Neurosci.* **26**, 193–198 (2003).
18. Dickendesher, T. L. *et al.* NgR1 and NgR3 are Receptors for Chondroitin Sulfate Proteoglycans. *Nat. Neurosci.* **15**, 703 (2012).
19. Gordon, J. A. & Stryker, M. P. Experience-dependent plasticity of binocular responses in the primary visual cortex of the mouse. *J. Neurosci.* **16**, 3274–3286 (1996).
20. Drager, U. C. Observations on monocular deprivation in mice. *J. Neurophysiol.* **41**, 28–42 (1978).
21. Fagiolini, M., Pizzorusso, T., Berardi, N., Domenici, L. & Maffei, L. Functional postnatal development of the rat primary visual cortex and the role of visual experience: Dark rearing and monocular deprivation. *Vision Res.* **34**, 709–720 (1994).
22. Oray, S., Majewska, A. & Sur, M. Dendritic spine dynamics are regulated by monocular deprivation and extracellular matrix degradation. *Neuron* **44**, 1021–1030 (2004).
23. Hensch, T. K. *et al.* Local GABA circuit control of experience-dependent plasticity in developing visual cortex. *Science (80-.).* **282**, 1504–1508 (1998).
24. Saiepour, M. H. *et al.* Ocular dominance plasticity disrupts binocular inhibition-excitation matching in visual cortex. *Curr. Biol.* **25**, 713 (2015).

25. Sawtell, N. B. *et al.* NMDA receptor-dependent ocular dominance plasticity in adult visual cortex. *Neuron* **38**, 977–985 (2003).
26. Frenkel, M. Y. & Bear, M. F. How monocular deprivation shifts ocular dominance in visual cortex of young mice. *Neuron* **44**, 917–923 (2004).
27. Kaneko, M., Stellwagen, D., Malenka, R. C. & Stryker, M. P. Tumor necrosis factor- α mediates one component of competitive, experience-dependent plasticity in developing visual cortex. *Neuron* **58**, 673–680 (2008).
28. Fagiolini, M. & Hensch, T. K. Inhibitory threshold for critical-period activation in primary visual cortex. *Nature* **404**, 183–186 (2000).
29. Iwai, Y., Fagiolini, M., Obata, K. & Hensch, T. K. Rapid Critical Period Induction by Tonic Inhibition in Visual Cortex. *J. Neurosci.* **23**, 6695–6702 (2003).
30. Fagiolini, M. *et al.* Specific GABAA circuits for visual cortical plasticity. *Science* (80-.). **303**, 1681–1683 (2004).
31. Huang, Z. J. *et al.* BDNF regulates the maturation of inhibition and the critical period of plasticity in mouse visual cortex. *Cell* **98**, 739–755 (1999).
32. Hanover, J. L., Huang, Z. J., Tonegawa, S. & Stryker, M. P. Brain-derived Neurotrophic Factor Overexpression Induces Precocious Critical Period in Mouse Visual Cortex. *J. Neurosci.* **19**, 1–5 (1999).
33. Chang, M. C. *et al.* Narp regulates homeostatic scaling of excitatory synapses on parvalbumin-expressing interneurons. *Nat. Neurosci.* **13**, 1090–1097 (2010).
34. Gu, Y. *et al.* Obligatory role for the immediate early gene NARP in critical period plasticity. *Neuron* **79**, 335–346 (2013).
35. Niell, C. M. & Stryker, M. P. Modulation of visual responses by behavioral state in mouse visual cortex. *Neuron* **65**, 472–479 (2010).
36. Fu, Y. *et al.* A cortical circuit for gain control by behavioral state. *Cell* **156**, 1139–1152 (2014).
37. Fu, Y., Kaneko, M., Tang, Y., Alvarez-Buylla, A. & Stryker, M. P. A cortical disinhibitory circuit for enhancing adult plasticity. *Elife* **4**, (2015).

38. Vetencourt, J. F. M. *et al.* The antidepressant fluoxetine restores plasticity in the adult visual cortex. *Science* **320**, 385–388 (2008).
39. Sale, A. *et al.* Environmental enrichment in adulthood promotes amblyopia recovery through a reduction of intracortical inhibition. *Nat. Neurosci.* **10**, 679–681 (2007).
40. Donato, F., Rompani, S. B. & Caroni, P. Parvalbumin-expressing basket-cell network plasticity induced by experience regulates adult learning. *Nature* **504**, 272–276 (2013).
41. Greifzu, F. *et al.* Environmental enrichment extends ocular dominance plasticity into adulthood and protects from stroke-induced impairments of plasticity. *Proc. Natl. Acad. Sci. U. S. A.* **111**, 1150–1155 (2014).
42. Gu, Y. *et al.* Neuregulin-Dependent Regulation of Fast-Spiking Interneuron Excitability Controls the Timing of the Critical Period. *J. Neurosci.* **36**, 10285–10295 (2016).
43. Pizzorusso, T. *et al.* Reactivation of Ocular Dominance Plasticity in the Adult Visual Cortex. *Science (80-.)*. **298**, 1248–1251 (2002).
44. Pizzorusso, T. *et al.* Structural and functional recovery from early monocular deprivation in adult rats. *Proc. Natl. Acad. Sci. U. S. A.* **103**, 8517 (2006).
45. D, C. *et al.* Animals lacking link protein have attenuated perineuronal nets and persistent plasticity. *Brain* **133**, 2331–2347 (2010).
46. McGee, A. W., Yang, Y., Fischer, Q. S., Daw, N. W. & Strittmatter, S. M. Experience-Driven Plasticity of Visual Cortex Limited by Myelin and Nogo Receptor. *Science (80-.)*. **309**, 2222–2226 (2005).
47. Stephany, C. É. *et al.* Plasticity of binocularity and visual acuity are differentially limited by nogo receptor. *J. Neurosci.* **34**, 11631–11640 (2014).
48. Trachtenberg, J. T., Trepel, C. & Stryker, M. Rapid extragranular plasticity in the absence of thalamocortical plasticity in the developing primary visual cortex. *Science (80-.)*. **287**, 2029–2032 (2000).
49. Liu, C.-H., Heynen, A., Shuler, M. & Bear, M. Cannabinoid Receptor Blockade Reveals Parallel Plasticity Mechanisms in Different Layers of Mouse Visual Cortex. *Neuron* **58**, 340–345 (2008).

50. Stephany, C.-E., Ikrar, T., Nguyen, C., Xu, X. & McGee, A. W. Nogo Receptor 1 Confines a Disinhibitory Microcircuit to the Critical Period in Visual Cortex. *J. Neurosci.* **36**, 11006–11012 (2016).
51. Pham, T. A. A semi-persistent adult ocular dominance plasticity in visual cortex is stabilized by activated CREB. *Learn. Mem.* **11**, 738–747 (2004).
52. Kuhlman, S. *et al.* A disinhibitory microcircuit initiates critical-period plasticity in the visual cortex. *Nature* **501**, 543–546 (2013).
53. Sun, Y. *et al.* Neuregulin-1/ErbB4 Signaling Regulates Visual Cortical Plasticity. *Neuron* **92**, 160–173 (2016).
54. Kim, J. E., Liu, B. P., Park, J. H. & Strittmatter, S. M. Nogo-66 receptor prevents raphespinal and rubrospinal axon regeneration and limits functional recovery from spinal cord injury. *Neuron* **44**, 439–451 (2004).
55. Wang, X. *et al.* Recovery from Chronic Spinal Cord Contusion after Nogo Receptor Intervention. *ANN NEUROL* **70**, 805–821 (2011).
56. Stephany, C.-É. *et al.* Distinct Circuits for Recovery of Eye Dominance and Acuity in Murine Amblyopia. *Curr Biol* **28**, 1914–1923 (2018).
57. Xu, X. *et al.* Primary visual cortex shows laminar-specific and balanced circuit organization of excitatory and inhibitory synaptic connectivity. *J. Physiol.* **594**, 1891–1910 (2016).
58. Dräger, U. C. Receptive fields of single cells and topography in mouse visual cortex. *J. Comp. Neurol.* **160**, 269–289 (1975).
59. Tsien, J. Z. *et al.* Subregion- and Cell Type–Restricted Gene Knockout in Mouse Brain. *Cell* **87**, 1317–1326 (1996).
60. Harris, J. A. *et al.* Anatomical characterization of Cre driver mice for neural circuit mapping and manipulation. *Front. Neural Circuits* **8**, 1–16 (2014).
61. Madisen, L. *et al.* A robust and high-throughput Cre reporting and characterization system for the whole mouse brain. *Nat. Neurosci.* **13**, 133–140 (2010).
62. Frantz, M. G. *et al.* Layer 4 Gates Plasticity in Visual Cortex Independent of a Canonical Microcircuit. *Curr. Biol.* 2962–2973 (2020) doi:10.1016/j.cub.2020.05.067.

63. Douglas, R. J. & Martin, K. A. C. Neuronal Circuits of the Neocortex. *Annu. Rev. Neurosci.* **27**, 419–451 (2004).
64. Freeman, R. D. & Olson, C. Brief periods of monocular deprivation in kittens: Effects of delay prior to physiological study. *J. Neurophysiol.* **47**, 139–150 (1982).
65. Lan, R. *et al.* Structure-activity relationships of pyrazole derivatives as cannabinoid receptor antagonists. *J. Med. Chem.* **42**, 769–776 (1999).
66. Crozier, R. A., Wang, Y., Liu, C. H. & Bear, M. F. Deprivation-induced synaptic depression by distinct mechanisms in different layers of mouse visual cortex. *Proc. Natl. Acad. Sci. U. S. A.* **104**, 1383–1388 (2007).
67. Howarth, M., Walmsley, L. & Brown, T. M. Binocular integration in the mouse lateral geniculate nuclei. *Curr. Biol.* **24**, 1241–1247 (2014).
68. Jaepel, J., Hübener, M., Bonhoeffer, T. & Rose, T. Lateral geniculate neurons projecting to primary visual cortex show ocular dominance plasticity in adult mice. *Nat. Neurosci.* **20**, 1708–1714 (2017).
69. Sommeijer, J. P. *et al.* Thalamic inhibition regulates critical-period plasticity in visual cortex and thalamus. *Nat. Neurosci.* **20**, 1716–1721 (2017).
70. Huh, C. Y. L. *et al.* Long-term Monocular Deprivation during Juvenile Critical Period Disrupts Binocular Integration in Mouse Visual Thalamus. *J. Neurosci.* **40**, 585–604 (2020).
71. Restani, L. *et al.* Functional Masking of Deprived Eye Responses by Callosal Input during Ocular Dominance Plasticity. *Neuron* **64**, 707–718 (2009).
72. Huberman, A. D. & Niell, C. M. What can mice tell us about how vision works? *Trends in Neurosciences* vol. 34 464–473 (2011).
73. Fournier, A. E., GrandPre, T. & Strittmatter, S. M. Identification of a receptor mediating Nogo-66 inhibition of axonal regeneration. *Nature* **409**, 341–346 (2001).
74. Schroeder, A. & De Wit, J. Leucine-rich repeat-containing synaptic adhesion molecules as organizers of synaptic specificity and diversity. *Exp. Mol. Med.* **50**, (2018).

75. Park, J. B. *et al.* A TNF receptor family member, TROY, is a coreceptor with Nogo receptor in mediating the inhibitory activity of myelin inhibitors. *Neuron* **45**, 345–351 (2005).
76. Mi, S. *et al.* LINGO-1 is a component of the Nogo-66 receptor/p75 signaling complex. *Nat. Neurosci.* **7**, 221–228 (2004).
77. Sekine, Y., Algarate, P. T., Cafferty, W. B. J. & Strittmatter, S. M. Plexina2 and CRMP2 signaling complex is activated by nogo-a-liganded ngr1 to restrict corticospinal axon sprouting after trauma. *J. Neurosci.* **39**, 3204–3216 (2019).
78. Wang, K. C., Kim, J. A., Sivasankaran, R., Segal, R. & He, Z. p75 interacts with the Nogo receptor as a co-receptor for Nogo, MAG and OMgp. *Nature* **420**, 74–78 (2002).
79. Baho, E. *et al.* p75 neurotrophin receptor activation regulates the timing of the maturation of cortical parvalbumin interneuron connectivity and promotes Juvenile-like plasticity in adult visual cortex. *J. Neurosci.* **39**, 4489–4510 (2019).
80. Smedfors, G., Olson, L. & Karlsson, T. E. A nogo-like signaling perspective from birth to adulthood and in old age: Brain expression patterns of ligands, receptors and modulators. *Front. Mol. Neurosci.* **11**, 1–14 (2018).
81. Hatanaka, Y. *et al.* Semaphorin 6A–Plexin A2/A4 Interactions with Radial Glia Regulate Migration Termination of Superficial Layer Cortical Neurons. *iScience* **21**, 359–374 (2019).
82. Prusky, G. T., West, P. W. R. & Douglas, R. M. Behavioral assessment of visual acuity in mice and rats. *Vision Res.* **40**, 2201–2209 (2000).
83. Prusky, G. T., Harker, K. T., Douglas, R. M. & Wishaw, I. Q. Variation in visual acuity within pigmented, and between pigmented and albino rat strains. *Behav. Brain Res.* **136**, 339–348 (2002).
84. Carulli, D. *et al.* Animals lacking link protein have attenuated perineuronal nets and persistent plasticity. *Brain* **133**, 2331–2347 (2010).
85. Carulli, D. *et al.* Composition of perineuronal nets in the adult rat cerebellum and the cellular origin of their components. *J. Comp. Neurol.* **494**, 559–577 (2006).

86. Morawski, M., Brückner, G., Arendt, T. & Matthews, R. T. Aggrecan : Beyond cartilage and into the brain. *Int. J. Biochem. Cell Biol.* **44**, 690–693 (2012).
87. Sorg, B. A. *et al.* Casting a wide net: Role of perineuronal nets in neural plasticity. *J. Neurosci.* **36**, 11459–11468 (2016).
88. Zimmermann, D. R. & Dours-Zimmermann, M. T. Extracellular matrix of the central nervous system: From neglect to challenge. *Histochem. Cell Biol.* **130**, 635–653 (2008).
89. Matthews, R. T. *et al.* Aggrecan Glycoforms Contribute to the Molecular Heterogeneity of Perineuronal Nets. *JN* **22**, 7536–7547 (2002).
90. Kind, P. C. *et al.* The development and activity-dependent expression of aggrecan in the cat visual cortex. *Cereb. Cortex* **23**, 349–360 (2013).
91. Lander, C., Kind, P., Maleski, M. & Hockfield, S. A family of activity-dependent neuronal cell-surface chondroitin sulfate proteoglycans in cat visual cortex. *J. Neurosci.* **17**, 1928–1939 (1997).
92. Guimarães, A., Zaremba, S. & Hockfield, S. Molecular and morphological changes in the cat lateral geniculate nucleus and visual cortex induced by visual deprivation are revealed by monoclonal antibodies Cat-304 and Cat-301. *J. Neurosci.* **10**, 3014–3024 (1990).
93. Dzyubenko, E., Gottschling, C. & Faissner, A. Neuron-Glia Interactions in Neural Plasticity: Contributions of Neural Extracellular Matrix and Perineuronal Nets. *Neural Plast.* **2016**, (2016).
94. Prabhakar, V. *et al.* Biochemical characterization of the chondroitinase ABC I active site. *Biochem. J.* **390**, 395–405 (2005).
95. Rowlands, D. *et al.* Aggrecan Directs Extracellular Matrix-Mediated Neuronal Plasticity. *J. Neurosci.* **38**, 10102–10113 (2018).
96. Giusti, S. A. *et al.* Behavioral phenotyping of Nestin-Cre mice: Implications for genetic mouse models of psychiatric disorders. *J. Psychiatr. Res.* **55**, 87–95 (2014).
97. Rittenhouse, E., Dunn, L. C. & Cookingham, J. Cartilage matrix deficiency (cmd): a new autosomal recessive lethal mutation in the mouse. *J. Embryol. Exp. Morphol.* **Vol. 43**, 71–84 (1978).

98. Watanabe, H. *et al.* Mouse cartilage matrix deficiency (cmd) caused by a 7 bp deletion in the aggrecan gene. *Nat. Genet.* **7**, 154–157 (1994).
99. Devienne, G. *et al.* Regulation of perineuronal nets in the adult cortex by the activity of the cortical network. *JN* **41**, 5790–5779 (2021).
100. Hippenmeyer, S. *et al.* A developmental switch in the response of DRG neurons to ETS transcription factor signaling. *PLoS Biol.* **3**, 0878–0890 (2005).
101. Stühmer, T., Puelles, L., Ekker, M. & Rubenstein, J. L. R. Expression from a Dlx gene enhancer marks adult mouse cortical GABAergic neurons. *Cereb. Cortex* **12**, 75–85 (2002).
102. Taniguchi, H. *et al.* A Resource of Cre Driver Lines for Genetic Targeting of GABAergic Neurons in Cerebral Cortex. *Neuron* **71**, 995 (2011).
103. Zhan, X. *et al.* Generation of BAF53b-Cre Transgenic Mice with Pan-Neuronal Cre Activities. *Genesis* **53**, 440 (2015).
104. W, H., K, B. & G, B. Wisteria floribunda agglutinin-labelled nets surround parvalbumin-containing neurons. *Neuroreport* **3**, 869–872 (1992).
105. Härtig, W., Meinicke, A., Michalski, D., Schob, S. & Jäger, C. Update on Perineuronal Net Staining With Wisteria floribunda Agglutinin (WFA). *Front. Integr. Neurosci.* **16**, 1–7 (2022).
106. Prusky, G. T. & Douglas, R. M. Characterization of mouse cortical spatial vision. *Vision Res.* **44**, 3411–3418 (2004).
107. Fawcett, J. W., Oohashi, T. & Pizzorusso, T. The roles of perineuronal nets and the perinodal extracellular matrix in neuronal function. *Nat. Rev. Neurosci.* **20**, 451–465 (2019).
108. Dityatev, A., Schachner, M. & Sonderegger, P. The dual role of the extracellular matrix in synaptic plasticity and homeostasis. *Nat. Rev. Neurosci.* **11**, 735–746 (2010).
109. Lensjø, K. K., Lepperød, M. E., Dick, G., Hafting, T. & Fyhn, M. Removal of perineuronal nets unlocks juvenile plasticity through network mechanisms of decreased inhibition and increased gamma activity. *J. Neurosci.* **37**, 1269–1283 (2017).

110. Deepa, S. S. *et al.* Composition of perineuronal net extracellular matrix in rat brain: a different disaccharide composition for the net-associated proteoglycans. *J. Biol. Chem.* **281**, 17789–800 (2006).

CURRICULUM VITAE

Emily C. Crouse, PhD
511 S. Floyd St., MDR Bldg, Room 438A
Louisville, KY, 40202
Phone: (270) 227-6612
eccrou01@louisville.edu

EDUCATION

2011-2015 B.A. in Psychology, Murray State University – Murray, KY
2017-2019 M.S. in Anatomical Sciences and Neurobiology, University of Louisville – Louisville, KY
2017-2023 Ph.D. in Anatomical Sciences and Neurobiology, University of Louisville – Louisville, KY

POSITIONS

2017 Graduate Research Assistant, University of Louisville, Louisville, KY
Laboratory of Dena Howland, PhD.
2018 – Graduate Research Assistant, University of Louisville, Louisville, KY
Laboratory of Aaron McGee, PhD.

PROFESSIONAL MEMBERSHIPS AND ACTIVITIES

2017- Society for Neuroscience, Louisville Chapter

HONORS AND AWARDS

2012-2013 CHA Housing Scholarship Recipient
Hope, Endeavor, Achievement Scholarship Recipient
Housing Scholarship Recipient
Regents Scholarship Recipient
Shroat Dunn Memorial Scholarship Recipient
KEES Scholarship Recipient
2013-2015 Hope, Endeavor, Achievement Scholarship Recipient
Regents Scholarship Recipient
Shroat Dunn Memorial Scholarship Recipient
KEES Scholarship Recipient

UNIVERSITY ACTIVITIES

2017 – Volunteer, Science Policy Outreach Group
2017 – Volunteer, Brain Days at the Kentucky Science Center

TEACHING ACTIVITIES

2019 - St. Francis Of Assisi Middle School Science Fair Tutor, Plant Electrophysiology
2019 6th grade – Iris Apple, 3rd place State Science Fair, Plant Sciences
2020 7th grade – Iris Apple, 2nd place State Science Fair, Plant Sciences
2021 8th grade – Iris Apple, 1st place State Science Fair, Plant Sciences
2019 Teaching Assistant, Neuroscience Gross Anatomy Lab, Fundamentals of Neuroscience
2020 Reviewer, Mock Study Session, Developmental Neurobiology
2021 Teaching Assistant, Synaptic Organization of the Central Nervous System

ORAL PRESENTATIONS

1. "Visual Acuity in Head-Fixed Behavior." McGee Lab Presentation, University of Louisville, February 2018.
2. "Experimental Models in Visual Plasticity." Anatomy Seminar, University of Louisville, October 2018.

3. "Fragile X Syndrome: A Switch from a Molecular Approach to a Circuit Approach." Anatomy Seminar, University of Louisville, February 2019.
4. "Electrophysiology in the McGee Lab." Anatomy Seminar, University of Louisville, June 2019.
5. "Deciphering the Role of CSPGs in Limiting Visual Plasticity." Proposal Defense, University of Louisville, August 2021.

PUBLICATIONS

Peer-reviewed Original Research Manuscripts

^ denotes co-authors

1. Frantz MG^, **Crouse EC^**, Sokhadze G^, Ikrar T, Stephany CE, Nguyen C, Xu X, and McGee AW. "Layer 4 gates plasticity in visual cortex independent of a canonical microcircuit." *Curr Bio*, 2020; 30(15): 2962–2973.
2. Boone HC, Samonds JM, **Crouse EC**, Barr C, Priebe NJ, and McGee AW. "Natural binocular depth discrimination behavior in mice explained by visual cortical activity." *Curr Bio*, 2021; 31(10): 2191–2198.